MARTIN MARIETTA ENERGY SYSTEMS LIBRARIES
3 4456 0365938 8

BRARY
ION

ORNL-3463
UC-34 – Physics
TID-4500 (29th ed.)

ELECTRON-SLOWING-DOWN SPECTRUM IN Cu OF BETA RAYS FROM Cu^{64}

W. J. McConnell
H. H. Hubbell, Jr.
R. D. Birkhoff

OAK RIDGE NATIONAL LABORATORY
operated by
UNION CARBIDE CORPORATION
for the
U.S. ATOMIC ENERGY COMMISSION

CENTRAL RESEARCH LIBRARY
DOCUMENT COLLECTION
LIBRARY LOAN COPY
DO NOT TRANSFER TO ANOTHER PERSON
If you wish someone else to see this document, send in name with document and the library will arrange a loan.

Printed in USA. Price: $1.75 Available from the
Office of Technical Services
U. S. Department of Commerce
Washington 25, D. C.

LEGAL NOTICE

This report was prepared as an account of Government sponsored work. Neither the United States, nor the Commission, nor any person acting on behalf of the Commission:

A. Makes any warranty or representation, expressed or implied, with respect to the accuracy, completeness, or usefulness of the information contained in this report, or that the use of any information, apparatus, method, or process disclosed in this report may not infringe privately owned rights; or

B. Assumes any liabilities with respect to the use of, or for damages resulting from the use of any information, apparatus, method, or process disclosed in this report.

As used in the above, "person acting on behalf of the Commission" includes any employee or contractor of the Commission, or employee of such contractor, to the extent that such employee or contractor of the Commission, or employee of such contractor prepares, disseminates, or provides access to, any information pursuant to his employment or contract with the Commission, or his employment with such contractor.

ORNL-3463

Contract No. W-7405-eng-26

HEALTH PHYSICS DIVISION

ELECTRON-SLOWING-DOWN SPECTRUM IN Cu OF BETA RAYS FROM Cu^{64}

W. J. McConnell
H. H. Hubbell, Jr.
R. D. Birkhoff

(Submitted as a thesis to the Faculty of the Graduate School of Vanderbilt University in partial fulfillment of the requirements for the degree of Master of Science in Physics.)

MAY 1964

OAK RIDGE NATIONAL LABORATORY
Oak Ridge, Tennessee
operated by
UNION CARBIDE CORPORATION
for the
U.S. ATOMIC ENERGY COMMISSION

MARTIN MARIETTA ENERGY SYSTEMS LIBRARIES
3 4456 0365938 8

ACKNOWLEDGMENTS

The author wishes to thank P. N. Hensley, R. S. Jones, and the staff of the Health Physics Machine Shop for their cooperation and help in this research.

The author also wishes to express his gratitude to the Oak Ridge Institute of Nuclear Studies for administering the Health Physics Fellowship which made possible his study at Vanderbilt University and his thesis work at the Oak Ridge National Laboratory.

TABLE OF CONTENTS

Page

ACKNOWLEDGMENTS ii

LIST OF TABLES vi

LIST OF FIGURES vii

I. INTRODUCTION 1

II. THEORY OF ELECTRON-SLOWING-DOWN 2

III. THE SPECTROMETER 5

A. Description
B. Energy Calibration
C. Line Profile and Resolution
D. Transmission and Effect of Faraday Cup Bias

IV. THE EXPERIMENT 22

A. Description of the Sources
B. Preparation of the Sources
C. Handling of the Sources After Activation
D. Measurement of Electron Flux

V. DATA ANALYSIS 30

A. Source Activity
B. Corona Discharge
C. Gamma-Ray Background
D. Grid Transmission
E. Keplertron Energy Window Correction
F. Correction for "Probe Area"
G. Correction for Positron Flux

VI. RESULTS 36

VII. CONCLUSIONS 40

APPENDIXES 41

I. SAMPLE CALCULATION OF ELECTRON FLUX 41

II. SOLID ANGLE SUBTENDED AT ONE HOLE BY THE REMAINING OPEN AREA OF CAVITY SOURCE 53

Page

III. FLUX NORMALIZATION FACTOR 55

A. Disk Source
B. Cavity Source

BIBLIOGRAPHY 57

LIST OF TABLES

Table Page

1. Spectro-Chemical Analysis of Copper Used for Making Sources . 23
2. Calculation of Electron Flux in Copper Containing Cu^{64} 48

LIST OF FIGURES

Figure		Page
1.	The Keplertron, a High Transmission, Low-Energy Beta Spectrometer	6
2.	The Keplertron	9
3.	Keplertron Transmission as a Function of Electron Energy for an Outer Sphere Potential of 10 V	13
4.	Keplertron Transmission as a Function of Electron Energy for an Outer Sphere Potential of 40 V	14
5.	Keplertron Transmission as a Function of Electron Energy for an Outer Sphere Potential of 227 V	15
6.	Keplertron Transmission as a Function of Electron Energy for an Outer Sphere Potential of 1450 V	16
7.	Keplertron Resolution as a Function of Electron Energy	17
8.	Keplertron Transmission Curves Without and With Inner Sphere Liner and Cup Bias	18
9.	Faraday Cup Current as a Function of Bias Potential	20
10.	Keplertron Transmission as a Function of Electron Energy	21
11.	Cavity Source, Platform, and Cover	24
12.	Electron Flux Spectrum of Cu^{64} Beta Rays Absorbed in Copper Plane Source	37
13.	Electron Flux Spectrum of Cu^{64} Beta Rays Absorbed in Copper Cavity Source	38
14.	Electron Stopping Power for Copper	52

I. INTRODUCTION

The understanding of the physical processes by which radiation interacts with matter involves a knowledge of the electron flux spectrum within the material. Measurements[1,2] of the electron flux spectrum arising from a beta-ray source uniformly distributed in a medium have been reported between 1.70 MeV and about 50 keV and represent the only data on the electron flux spectrum resulting from the slowing down of electrons in infinite, uniform, homogenous, and isotropic media. These measurements have shown good agreement with a simplified version of the continuous-slowing-down theory of Spencer and Fano[3]. However, the region below 50 keV has remained unexplored up to this time. A knowledge of the electron flux spectrum in this region would be of considerable value because large fluxes result from secondary electron production and because these electrons have higher cross sections for interaction with matter than do electrons of higher energies.

The purpose of the work described here was to measure the electron flux over this important region. It is hoped that these and future measurements of the electron flux produced by other ionizing radiations will clarify the physical mechanisms which result in the differing biological effectivenesses of the various types of ionizing radiations.

---

[1] R. D. Birkhoff, H. H. Hubbell, Jr., J. S. Cheka, and R. H. Ritchie, Health Physics 1, 27 (1958).

[2] R. D. Birkhoff and W. H. Wilkie, Bull. Am. Phys. Soc. 8, 391.

[3] L. V. Spencer and U. Fano, Phys. Rev. 93, 1172 (1954).

II. THEORY OF ELECTRON SLOWING DOWN

A method for calculating the electron flux at any energy above a few keV due to the slowing down of primary and secondary electrons has been given by Spencer and Fano.[4] A simplified treatment of the theory has been given by Spencer and Attix[5] and reviewed by Birkhoff.[6] Flux calculations by the use of the Spencer-Fano theory and performed on the digital computer have been tabulated in a recent National Bureau of Standards publication.[7] In the treatment by Spencer and Fano the approximation to the primary electron flux spectrum (in which the flux at energy T is given by the number of primary electrons above T divided by the stopping power at T) is modified by considering the secondary electrons produced by the few violent collisions experienced by the primary electrons as an additional source and by considering the large energy losses due to bremsstrahlung as a "negative source".

For a uniform, isotropic, non-monochromatic electron source producing N(T) electrons cm^{-3} eV^{-1} sec^{-1} with energies between T and T + dT, the electron flux y(T) is given by

---

[4] Ibid.

[5] L. V. Spencer and F. H. Attix, Rad. Res. 3, 239 (1955), see also National Bureau of Standards Handbook 79, footnote 11, p. 20.

[6] R. D. Birkhoff, in Handbuch der Physik, edited by S. Flügge (Springer-Verlag, Berlin, 1958), Vol. 34, p. 53.

[7] R. T. McGinnies, National Bureau of Standards Circular No. 597, 1959.

$$y(T) = \left[\int_T^{T_o} \bar{K}_c\ (T', T)\ dT' + \int_T^{T_o} \bar{K}_b\ (T', T)\ dT'\right]^{-1}$$

$$\left\{ \int_T^{T_o} N(T')\ dT' + \int_{2T}^{T_o} K_s(T', T)\ y(T')\ dT' - \int_{2T}^{T_o} K_b(T', T)\ y(T')\ dT' \right.$$

$$- \int_T^{\Delta} \left(\left[K_c(T', T) + \bar{K}_b\ (T', T)\right] y(T') \right.$$

$$\left. \left. - \left[\bar{K}_c(t', t) + \bar{K}_b\ (t', t)\right] y(t) \right) \right\} \tag{1}$$

where $\Delta = 2T$ or T_o whichever is smaller,

$$\bar{K}_c(T', T) = (2\pi\ m_o c^2\ N_e r_o^{\ 2}/\beta^2)\ \left\{(T' - T)^{-1} - T + (T + 1)^{-2}\right.$$

$$\left.(T - T'/2)\right\} \tag{2}$$

$$\bar{K}_b(T', T) = m_o c^2\ Z\ N_e r_o^{\ 2}/137)\left[28.1 - (16/9)\ \ln Z\right] \times \left[T/(T + 1)\right]$$

$$\ln\left[T'/(T' - T)\right] \tag{3}$$

$$K_s(T', T) = (2\pi\ m_o c^2\ N_e r_o^{\ 2}/\beta'^2)\left\{T^{-1} - (T' - T)^{-1} + (T' + 1)^{-2}\right.$$

$$\left.(T'/2 - T)\right\} \tag{4}$$

$$K_b(T', T) = (m_o c^2\ ZN_e r_o^{\ 2}/137)\left[28.1 - (16/9)\ \ln Z\right] \times \left[T'/(T' + 1)\right]$$

$$\ln\left[T'/(T' - T)\right] \tag{5}$$

and

$$K_c(T', T) = (2\pi\ m_o c^2\ N_e r_o^{\ 2}/\beta')\ \left\{(T' - T)^{-1} - T^{-1} - T^{-1} + (T' + 1)^{-2}\right.$$

$$\left.(T - T'/2)\right\} \tag{6}$$

where $m_o c^2$ is the electron rest energy, r_o is the classical electron radius; N_e and Z are the electron density and atomic number, respectively, of the absorbing material, $\beta = \frac{v}{c}$ measures the velocity of the electron, and T_o is the energy of the most energetic electron in the medium.

The term in $[\quad]^{-1}$ in equation 1 represents a stopping power. The first three terms in $\{\ \}$ in equation 1 represent a "source" of electrons from nuclear decay, violent collisions and bremsstrahlung, respectively. The last two terms in $\{\ \}$ in equation 1 represent the electrons which "jump" over the energy level being considered due to violent collisions and bremsstrahlung losses, respectively.

If the absorption occurs in a material of low atomic number and the initial electron energies are less than one MeV, bremsstrahlung may be neglected, and y(T) may be approximated[8] by

$$y(T) = \left[S_z(T)\right]^{-1}\left\{\int_T^{T_o} N(T')\ dT' + \int_{2T}^{T_o} K_s(T', T)\ y(T')\ dT'\right\} \qquad (7)$$

where S_z is the stopping power of the absorbing medium.

A calculation of the electron flux in copper containing Cu^{64} is given in Appendix 1.

---

[8] L. V. Spencer and F. H. Attix, loc. cit.

III. THE SPECTROMETER

A. Description

Measurements of the electron flux were made with the "Keplertron", a spherical, electrostatic-focusing spectrometer. An inverse square electric field between two concentric, charged spheres provides a focusing for electrons which leave a source on the inner sphere. This inverse square field causes the electrons to move in Kepler orbits, hence the name Keplertron. After energy analysis, the electrons enter a field free region where they are detected as a current. A schematic diagram of the Keplertron is shown in Figure 1. Since detailed discussions on the theoretical characteristics of the Keplertron have been given elsewhere,[9,10] only those characteristics pertinent to source design and Keplertron calibration are given here.

For a point source, the transmission T (defined as the ratio of the number of monoenergetic electrons which arrive at the detector to those which left the source) is given by

$$T = \frac{\chi}{4} \tag{8}$$

where χ is the supplement of the central angle through which the electrons rotate while in the inverse square field and is measured in radians. The energy resolution $\delta_{\frac{1}{2}}$ (defined as the width of the line profile at half height divided by the energy) is given by

---

[9] R. H. Ritchie, J. S. Cheka, and R. D. Birkhoff, Nuclear Instr. and Methods 6, 157 (1960).

[10] R. D. Birkhoff, J. M. Kohn, H. B. Eldridge, and R. H. Ritchie, Nuclear Instr. and Methods 8, 313 (1960).

UNCLASSIFIED
ORNL-LR-DWG. 67356

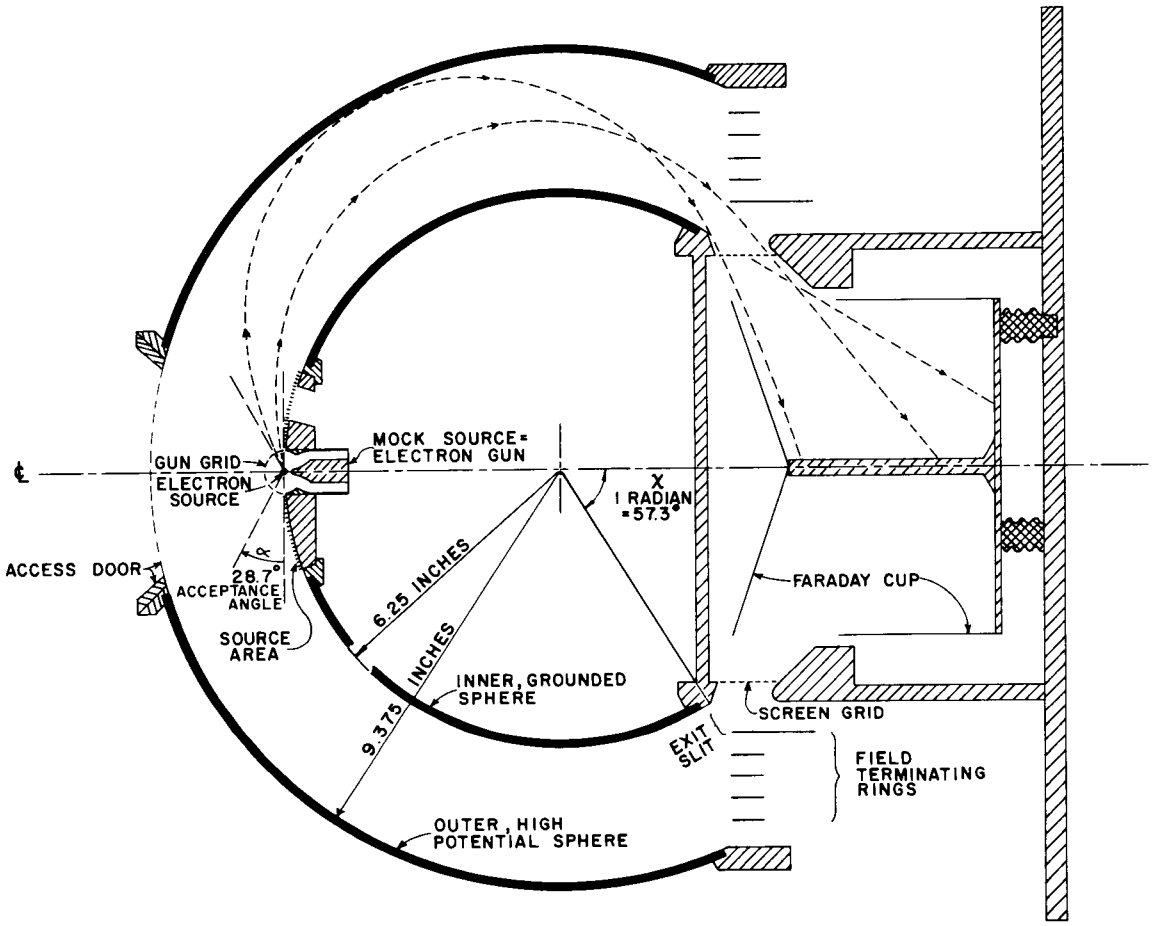

Fig. 1. The Keplertron, a High Transmission, Low-Energy Beta Spectrometer.

$$\delta_{\frac{1}{2}} = \frac{X^2}{16} \tag{9}$$

The line profile consists of two intersecting curves. The equations of these curves are:

$$T(\delta) = \frac{1}{4}\{X^2 + 16\delta\}^{\frac{1}{2}} \quad -\frac{X^2}{16} \leq \delta \leq 0 \tag{10}$$

and

$$T(\delta) = \frac{1}{4}\{X - (16\delta)^{\frac{1}{2}}\} \quad 0 \leq \delta \leq \frac{X^2}{16} \tag{11}$$

where

$$\delta = \frac{E - E_o}{E_o} \tag{12}$$

The electron energy E_o is determined by the sphere sizes and voltage between the two spheres and is given by

$$E_o = \{\frac{r_e}{2(r_e - r_m)}\} V_o \tag{13}$$

where V_o is the potential difference between the spheres, r_e is the radius of the outer sphere, and r_m is the radius of the inner sphere.

The main requirement desired of the Keplertron is that it have a high transmission. For this reason the value of the angle X was chosen as 1 radian. The value gives a theoretical transmission of 25% and an acceptable value of 6.3% for the theoretical energy resolution. With this choice of X, all electrons whose energies satisfy Equation (13) and which are emitted at any azimuth and within an angular range from 0° to 28.6^o to the plane tangent to the inner sphere at the source position pass through the exit slit. Because of this high transmission, a Faraday cup and an electrometer are used as a detector instead of the more conventional Geiger counter, thus allowing operation at electron energies below those required to penetrate a counter window.

The size of the Keplertron is determined by the inside dimensions of an available vacuum tank which has a diameter of about 27 in. The tank is equipped with compensating coils which reduce the earth's magnetic field in the region of the Keplertron to about 30 milligauss. Because the electrometer must be at ground potential, the focusing potential is applied to the outer sphere. To reduce the possibility of corona discharge, the outer sphere is placed midway (geometrically) between the inner sphere and tank wall. To conform to this requirement and to provide space between the spheres to accept all trajectories contributing to the 25% transmission, the outer sphere radius is 9.375 in. and the inner sphere radius is 6.25 in. This gives a theoretical energy calibration of $E_o = 1.50\ V_o$.

The spheres are made of 1/8-in. brass rods converging on the source as shown in Fig. 2. Rods are used instead of solid spheres to minimize the number of electrons scattered from the spheres into the exit slit. Aluminum or magnesium rods would have been preferred because of their lower atomic numbers, but were not readily available in alloys of sufficient elasticity to make accurate spheres. Also, it was feared that the oxide coatings of these metals would not provide good equipotential surfaces.

Five aluminum field-terminating rings are used to preserve the inverse square field near the slit. The ring nearest the inner sphere and the inner sphere form the edges of the exit slit which has a width of 0.8 in. The potential of each ring is held to the value appropriate to its location between the spheres by connection to a tap on a 370-

Fig. 2. The Keplertron.

megohm potential divider between the spheres. The current in this calibrated divider is also used to measure the outer sphere voltage, as explained in Section IV, Part D. A grid made of fine gold wires is placed just beyond the exit slit to reduce the capacitance between the outer sphere and the Faraday cup. The capacitance measured with the grid in place is 4.1×10^{-15}f. The transmission calculated from the geometrical area of the exit slit obstructed by the grid and supports is 0.96. This grid was used for the electron flux measurements. A cruder grid of aluminum wires was used to make the calibration measurements described below. The measured capacitance and transmission with this grid were 4.7×10^{-16}f and 0.40, respectively. The measurements below were corrected for the grid transmission.

B. Energy Calibration

The energy calibration was checked from 1.5 eV to about 3 keV using an electron gun in the source position. Below 20 eV the energy spread of electrons from the filament made interpretation of data difficult and above 3 keV corona discharge inside the gun prevented further measurements. The heating current in the filament produced a potential drop of about 2 V along the emitting region, and thus the emitted electrons had at least this great an energy spread. Several guns were made in an effort to achieve isotropic emission which would simulate a radioactive source. One design consisted of a tungsten ball 0.2 in. in diameter heated internally by a double- wound, tungsten, helical filament. The ball was at the center of a 0.75 in. diameter hemispherical grid of gold wires. However, it proved impossible to

heat the ball hot enough to clean the surface or to obtain an emission greater than 10^{-10} amperes. Instead, the data described here were obtained with an electron source consisting of a 0.100-in. diameter, circular filament of 0.002-in. tungsten wire at the center of the hemispherical gold grid.

The energy calibration determined by a least squares fit to fifty-five electron gun data points was found to be

$$E_o = 1.194 \pm 0.014 + (1.3710 \pm 0.0002)V_o \tag{14}$$

where the constant $- 1.194 \pm 0.014$ probably represents the contact potential between the filament and grid, E_o is the electron energy in eV, and V_o is the outer sphere potential in volts. The errors given in Equation 15 are probable errors. The possibility of an undetected systematic error is not excluded. The energy calibration was also checked using the Sm^{152} KLL Auger line at 31.4 keV resulting from K-capture in a Eu^{152} source of thickness 50 $\mu g/cm^2$ and found to be $E_o = (1.37 \pm 0.01)V_o$, where the error stated is an estimated error. The reason for the difference between the experimental calibration and the theoretical calibration ($E_o = 1.50V_o$) is not known, but it is thought that field leakage through the rods comprising the spheres may have been responsible.

C. Line Profile and Resolution

Line profiles obtained with the electron gun previously described had the theoretical shape except at low energies where the thermionic energy spread of electrons from the filament was significant. Although not enough data are available for a detailed comparison, the line profile

of the Sm^{152} Auger line appears to be in satisfactory agreement with theory. Line profiles at 13.7 eV, 54.8 eV, 311 eV, and 1990 eV are shown in Figures 3, 4, 5, and 6, respectively.

The resolution measured using the electron gun agrees with the theoretical value of 6.3% for energies greater than 50 eV. The Sm^{152} Auger line gave a resolution of $(7 \pm 1)\%$. Figure 7 shows the resolution as a function of electron energy. The deviations at low energies are assumed to be due to the spread in energy of electrons from the electron gun.

D. Transmission and Effect of Faraday Cup Bias

Figure 8a shows the first transmission curve made with the Keplertron and electron gun. The line has the theoretical shape for 1990-eV electrons, but there is also a large, spurious peak apparently due to electrons with lower energies. These appeared to be electrons which were repelled into and traversed the inner sphere with subsequent deflection into the Faraday cup.

Also, the transmission at the peak was lower than expected. This fact was attributed to electrons escaping through the large entrance slit of the Faraday cup.

Figure 8b shows the effect of lining the inside of the inner sphere with aluminum foil and applying a bias potential between the Faraday cup and the exit slit grid. The ratio of the line peak to the spurious peak was more than doubled, the spurious peak was much narrower, and the area of the spurious peak was only about 10% the area of the line peak.

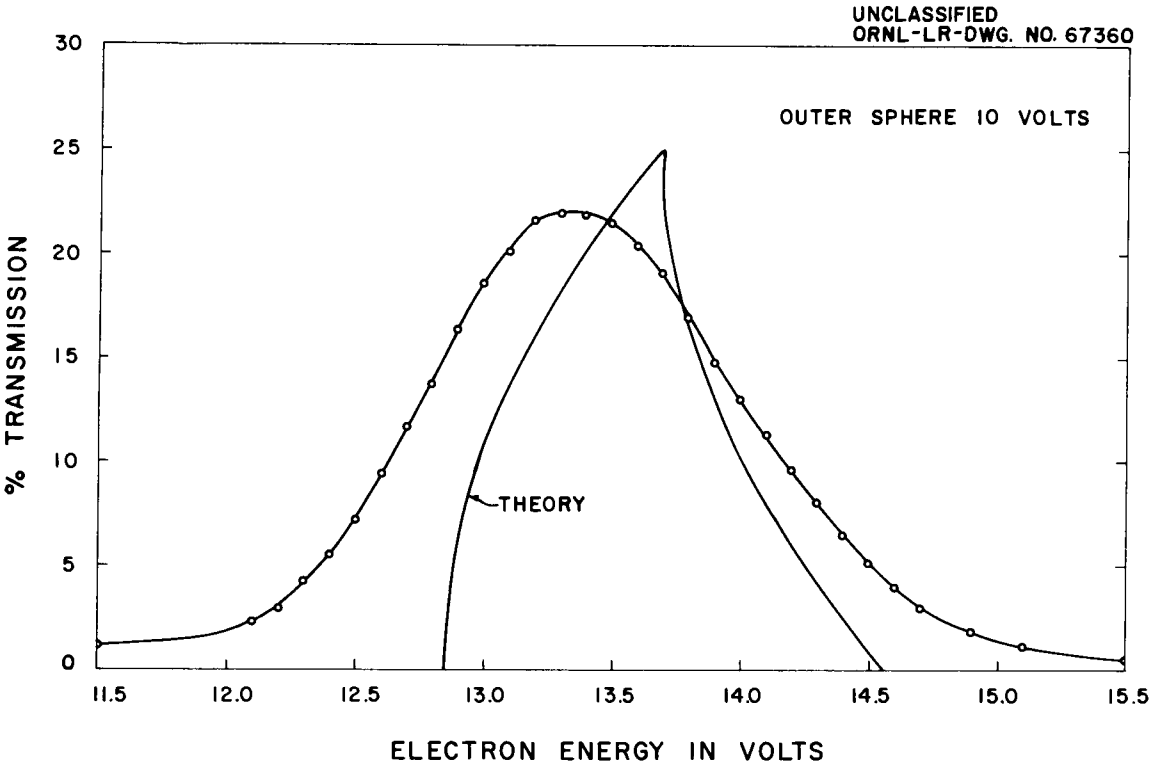

Fig. 3. Keplertron Transmission as a Function of Electron Energy for an Outer Sphere Potential of 10 V.

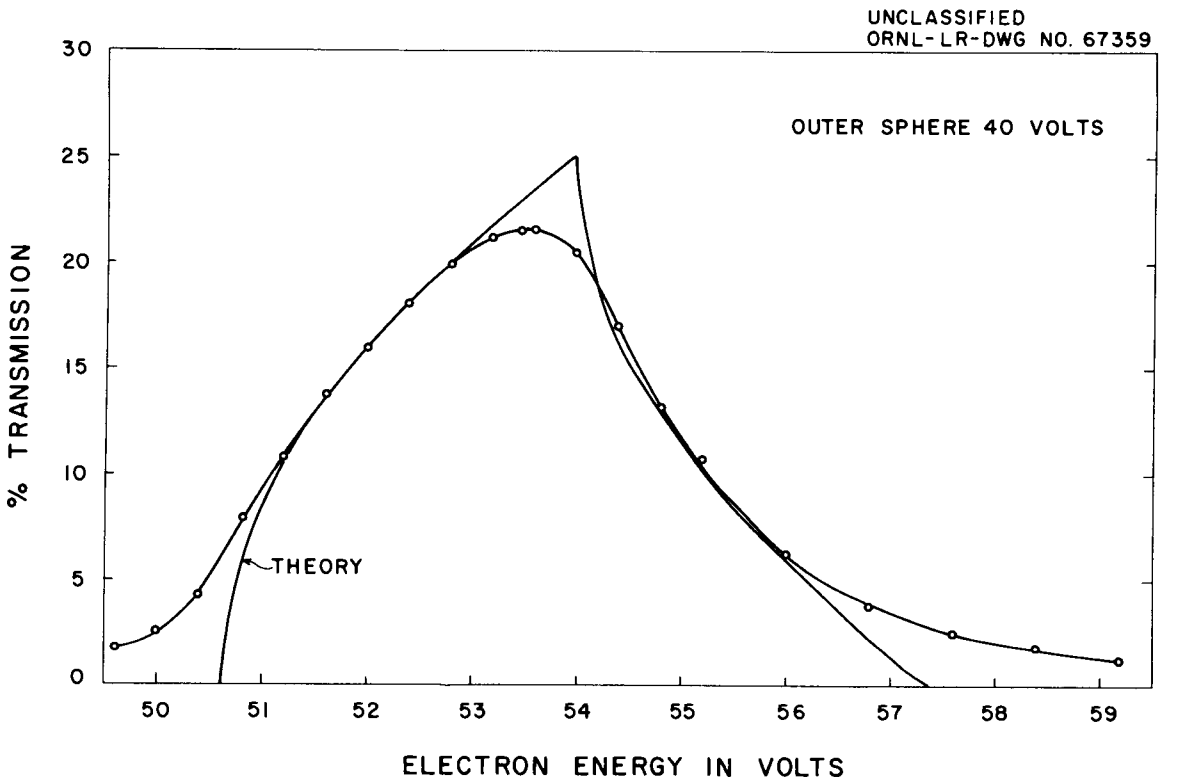

Fig. 4. Keplertron Transmission as a Function of Electron Energy for an Outer Sphere Potential of 40 V.

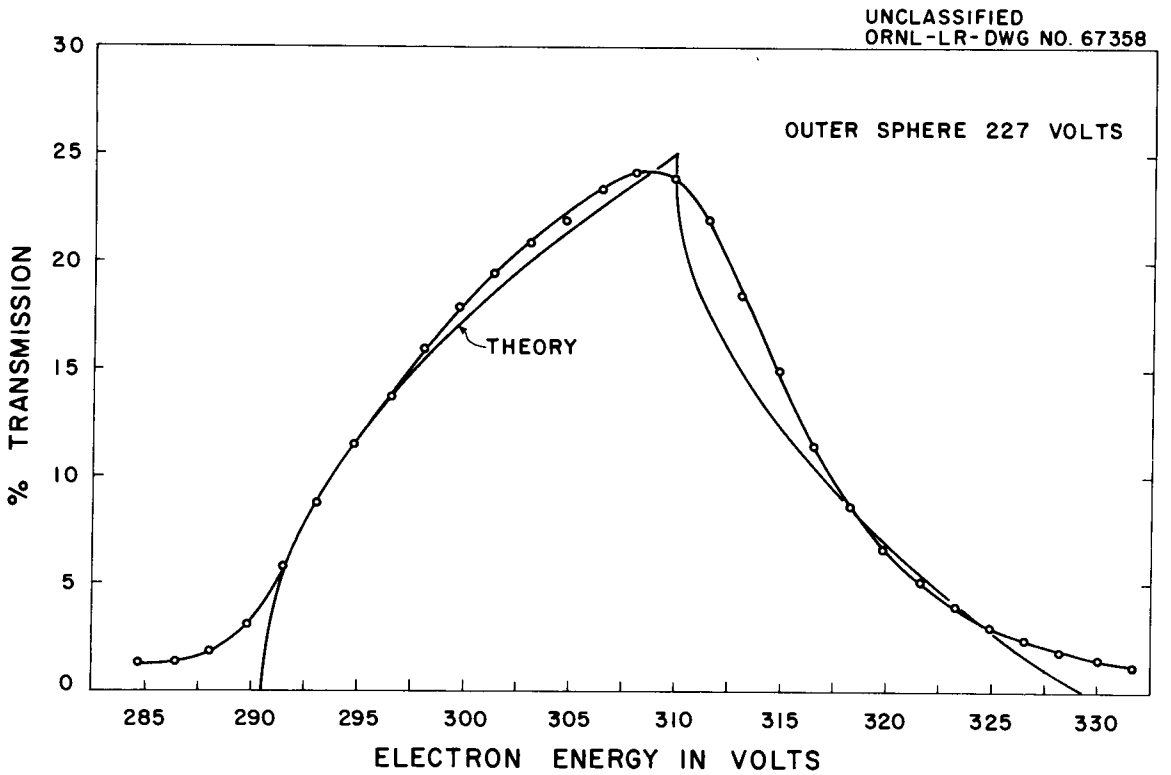

Fig. 5. Keplertron Transmission as a Function of Electron Energy for an Outer Sphere Potential of 227 V.

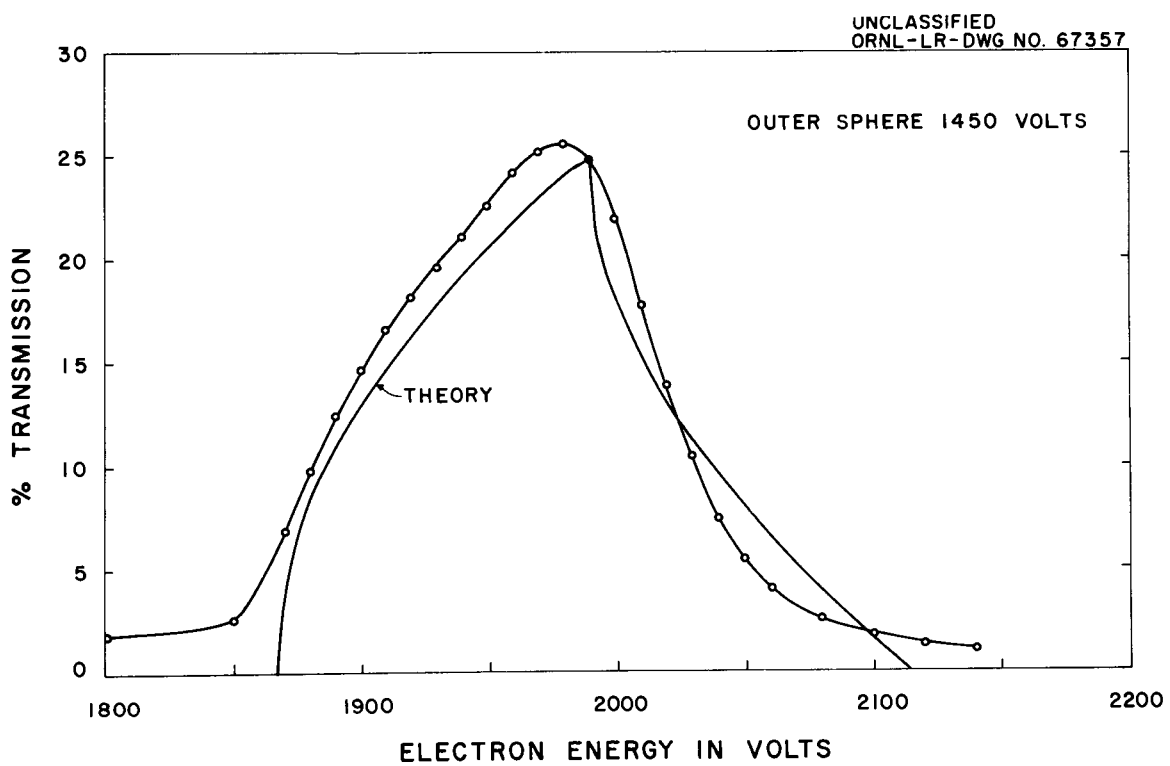

Fig. 6. Keplertron Transmission as a Function of Electron Energy for an Outer Sphere Potential of 1450 V.

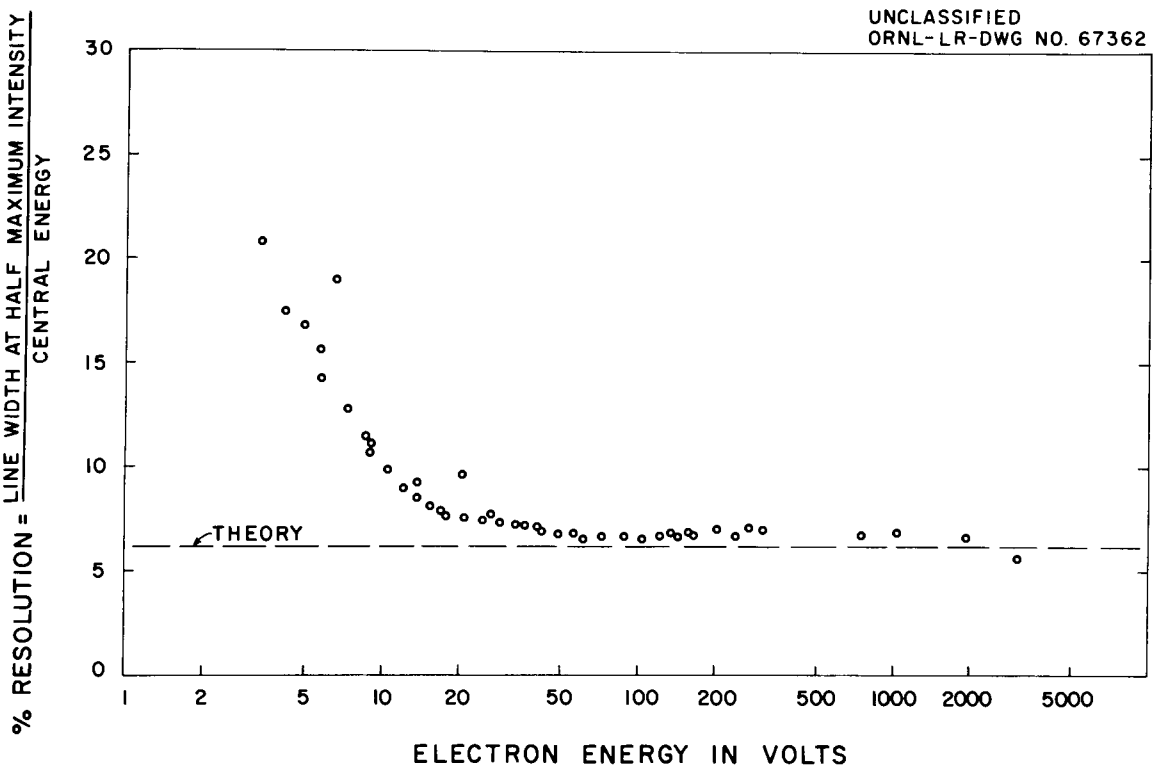

Fig. 7. Keplertron Resolution as a Function of Electron Energy.

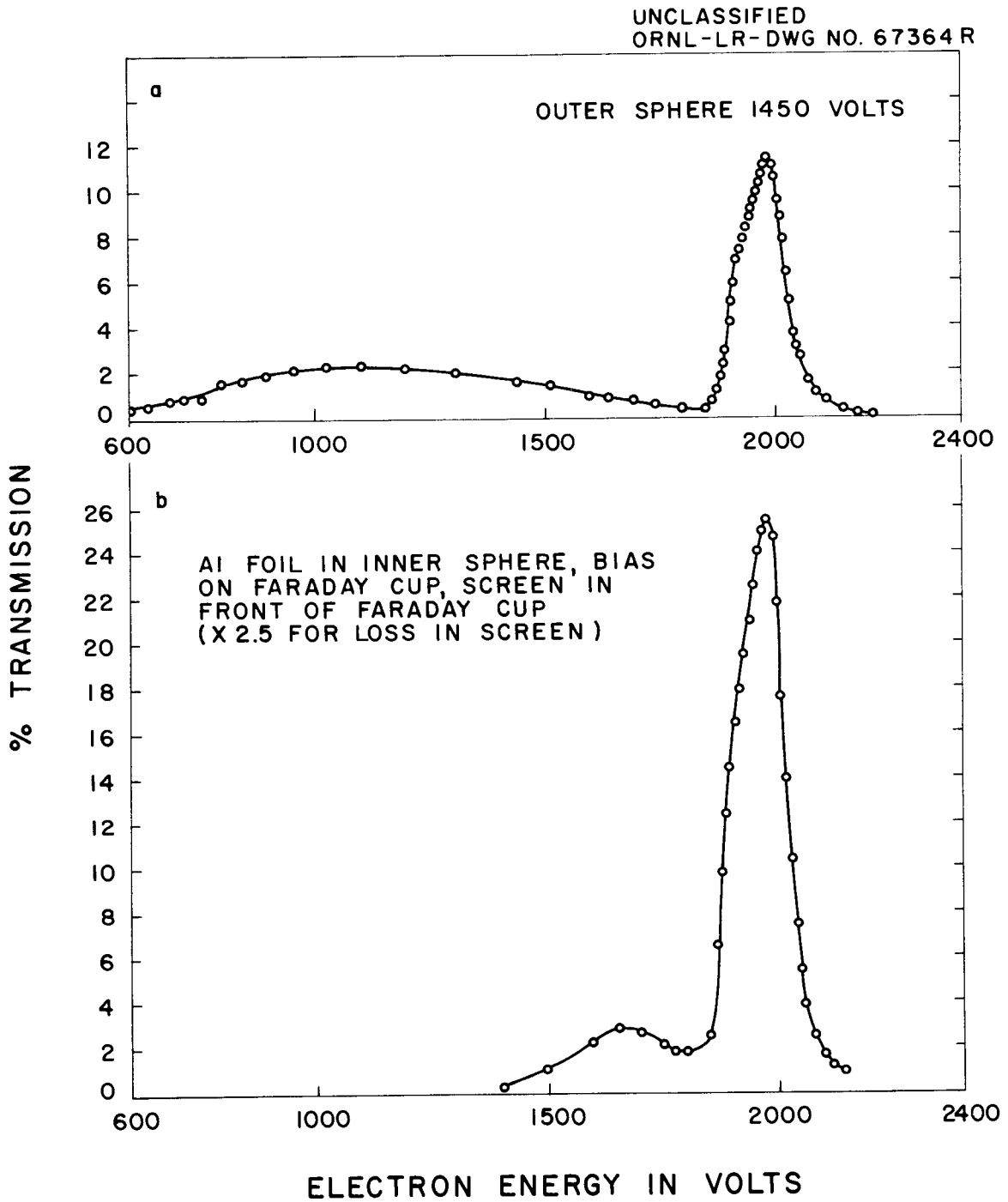

Fig. 8. Keplertron Transmission Curves Without and With Inner Sphere Liner and Cup Bias.

Figure 9 shows the cup current as a function of bias potential. Since saturation occurred at nearly the same potential for all incident electron energies between 12.3 V and 311 V, it was concluded that the bias was preventing the escape of electrons rather than attracting spurious electrons to the cup. Bias potentials greater than 20 V were used in the experiments described here. At this potential all curves are well into the saturation plateau.

The transmission measured using the electron gun agrees with the theoretical value of 25% for energies greater than 50 eV. The Sm^{152} Auger line gave a transmission of $(25 \pm 7)\%$. Figure 10 shows the transmission at maximum current as a function of electron energy. Again, the deviations at low energies are assumed to be due to the spread in energy of electrons from the electron gun. The bars represent probable errors.

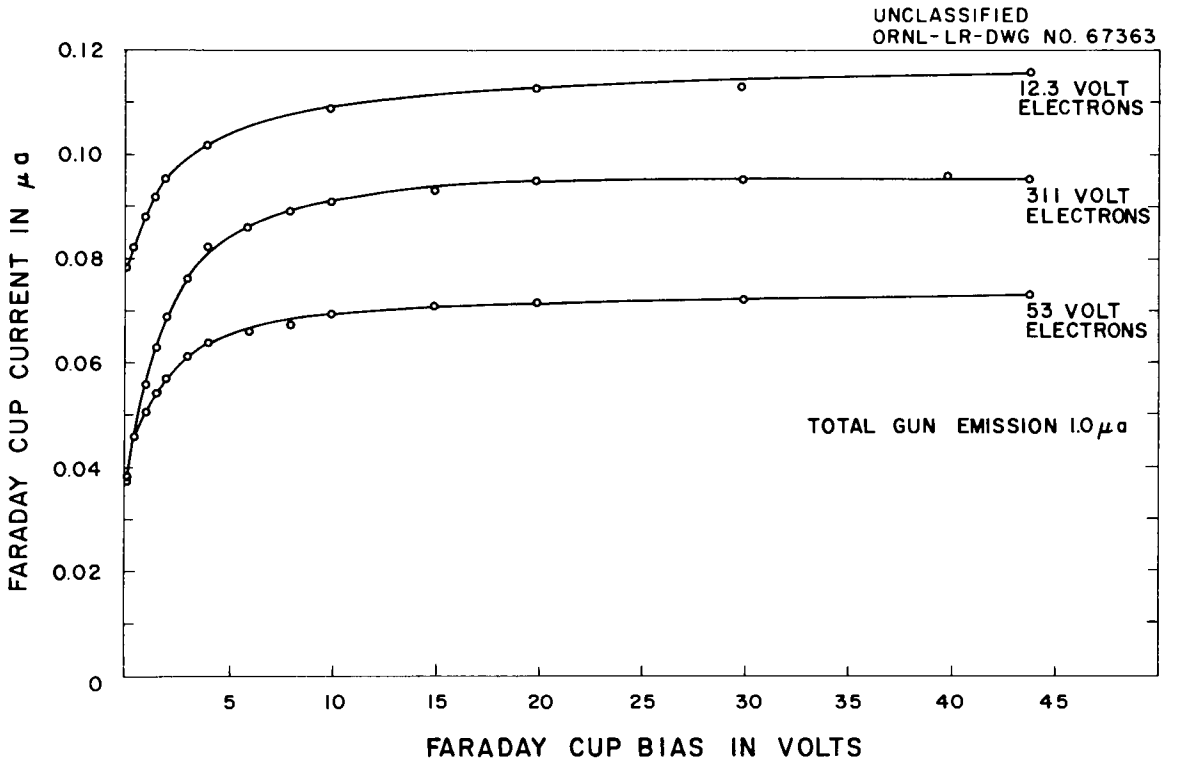

Fig. 9. Faraday Cup Current as a Function of Bias Potential.

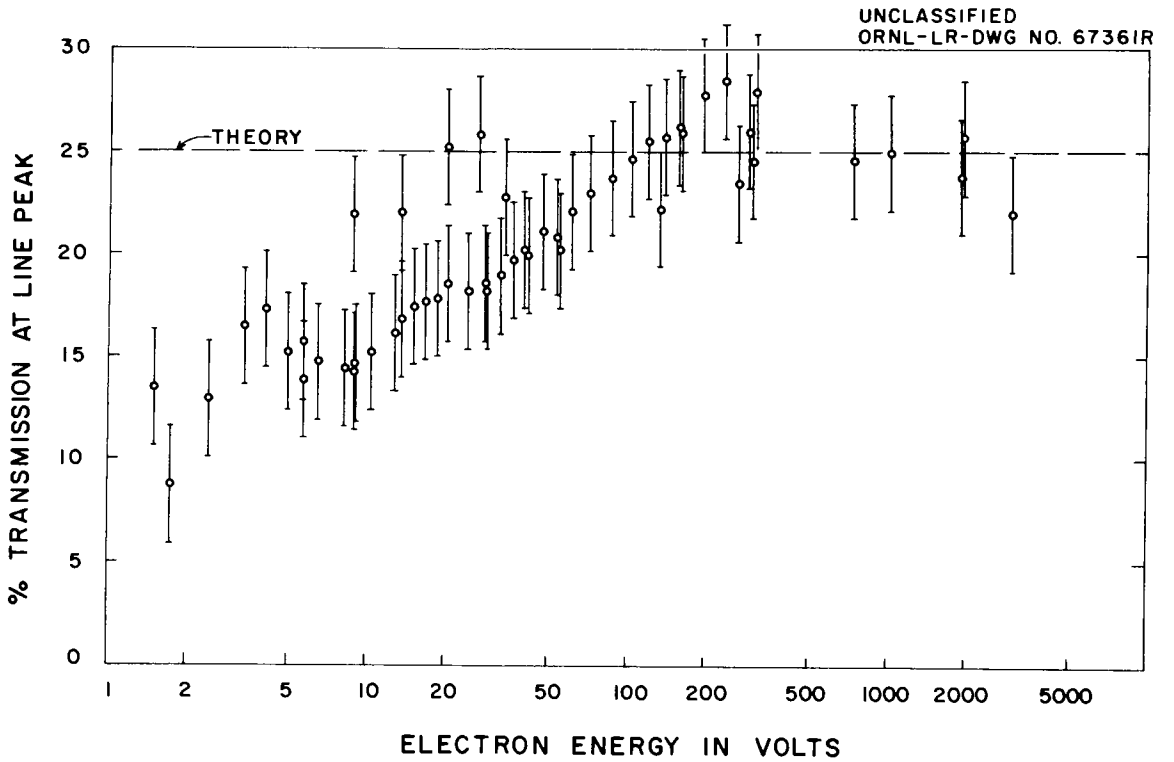

Fig. 10. Keplertron Transmission as a Function of Electron Energy.

IV. THE EXPERIMENT

A. Description of the Sources

Electron flux measurements were made using two types of sources, a plane disk source and a "black body cavity" source. Both sources were machined from very pure, (see Table 1 for analysis) stable copper obtained from the ORNL Metallurgy Division and activated in a reactor to produce a uniform distribution of radioactivity within the material. The disk source was irradiated for 48 hours in a flux of 6×10^{12} thermal neutrons cm^{-2} sec^{-1} and the cavity source for 2 hours in a flux of 2×10^{14} thermal neutrons cm^{-2} sec^{-1}.

The disk source consisted of a plane copper disk with a screw on one side. It was similar in appearance to the platform shown in Figure 11 but without the projecting fins. The total mass was 0.7 g. The diameter of the disk was 1.10 cm and the thickness of the disk was 0.050 cm. Since the maximum range of a 657-keV positron in copper is 0.043 cm, the disk was infinitely thick for the Cu^{64} positrons and negatrons with end-point energies of 657 keV and 571 keV, respectively. The screw served only to secure the disk to a mount and was surrounded by the mount. Thus, the screw did not contribute to the electron flux. However, since the screw accounted for about one-half of the mass of the source, it did make a considerable contribution to the gamma-ray activity and increased the difficulties involved in source handling.

The cavity source (Figure 11) was a hollow copper frustrum with walls 0.05 cm thick, which had a height of 0.73 cm, an outer diameter of 1.50 cm at the base, and an outer diameter of 1.15 cm at the top.

TABLE 1

SPECTRO-CHEMICAL ANALYSIS* OF COPPER
USED FOR MAKING SOURCES

Element	Composition by Weight (%)
Cu	> 99.999
Fe	< 0.00007
Sb	< 0.0001
Sn	< 0.0001
Pb	< 0.0001
Ni	< 0.0001
Bi	< 0.00001
Ag	< 0.00003
As	< 0.0002
Cr	< 0.00005
Si	< 0.00001
Te	< 0.0002
Se	< 0.0001
S	< 0.0001

Activation Analysis 104 Days After Irradiation

Co	< 0.001

---

*Supplied by R. E. Reed, Metallurgy Division, ORNL.

Fig. 11. Cavity Source, Platform, and Cover.

The total mass was 1.3 g. There were two rows of twelve holes each through the curved surface of the frustrum. The holes in the upper row had diameters of 0.28 cm and those in the lower row had diameters of 0.30 cm. The fractional solid angle subtended at one hole by the other twenty-three holes was calculated to be approximately 0.16, thus insuring that any given hole "looked" into a black body cavity. The calculation is given in Appendix II. The outside of the curved surface was at an angle of 14.3° from the normal to the base. This angle was chosen so electrons which emerged from the holes entered the 0° to 28.6° angular acceptance range of the Keplertron as near the center of the range as possible. The value of 28.6° was chosen for the angle between the base and the diagonal from one edge of the base to the opposite side of the top. This angle was chosen to permit all points on the base the same geometrical opportunity to radiate into the angular aceptance range of the Keplertron. The choice of these two angles determined the relationship that the height was approximately equal to the radius of the base. To insure that only electrons which originated inside the cavity reached the spectrometer, a brass cover (Figure 11) was placed over the source. The walls of the cover were 0.05 cm thick. The cover had two rows of holes whose centers were common to the holes in the source. The holes in the upper row had diameters of 0.25 cm and those in the lower row had diameters of 0.28 cm. The sizes of these holes were determined by the requirement that the sides of the holes in the source not radiate into the angular acceptance range of the Keplertron.

B. Preparation of the Sources

Prior to activation, the radiating surfaces of both sources were cleaned to remove cutting oil and oxide layers. The disk source was washed with acetone and water, then polished with sapphire dust and distilled water while in a nitrogen atmosphere. Without being removed from the nitrogen atmosphere the source was loaded in a source container ("rabbit"). A lead gasket was used to seal the lid of the rabbit.

The cavity source was washed with trichloroethylene, ethyl alcohol, and water, hydrogen annealed above 300° C for about 16 hours, and sealed in a helium atmosphere prior to activation.

C. Handling of the Sources After Activation

Because the detector was a current measuring device, sources were required whose activities were large compared to those usually encountered in beta spectroscopy. Both sources used in this work had activities of several curies. The gamma doses were about 16 r/hr at one foot for the disk source and about 33 r/hr at one foot for the cavity source. As a result, the sources required handling techniques different than those usually employed in beta spectroscopy.

The cavity source was assembled in a "hot cell". The source was removed from its sealed container and placed on a platform (Figure 11) which has been pre-screwed into a mount. The cover was then placed over the source. Small fins which projected from the platform and fitted into slots in the source and cover served to align the holes. The mount and covered source were placed in a lead container and transported to the Keplertron.

A different procedure was used for the disk source. The rabbit was decapped in the open and emptied behind a lead brick barricade. The source was then picked up using a special tool and screwed into the mount. This method has since been abandoned because too much time was wasted in picking up the source and aligning the screw with the mount. Also, the dose received in the decapping operation was considered unnecessarily high. Modification of existing tools and construction of new tools has eliminated these problems. A snap fastener has been substituted for the screw. A lucite block and removable lucite funnel to align the source and mount have been made. A new lead container and matching decapping tool have been made. An insert which holds the source with the snap side upward has been made for the rabbits.

The procedure now in use is to decap the rabbit while it is still in the lead container. The source is removed from the rabbit using a special tool and placed on the lucite block using the funnel as a guide. The funnel is removed and the mount is aligned by means of a cylindrical hole in the block and pushed against the source until the two snap together. The mount and source are then placed in another lead container and transported to the Keplertron.

D. Measurement of Electron Flux

The sources were placed on the inner sphere of the Keplertron and measurements of the electron flux were obtained by varying the outer sphere potential. Currents of 1.8×10^{-14} amp to 3.8×10^{-13} amp for the disk source and 1.1×10^{-13} amp to 4.4×10^{-12} amp for the cavity

source were observed after backgrounds described in Section V, Part C were subtracted. The observed current remained nearly constant because the electron flux was proportional to E^{-1} while the "window width" of the Keplertron was proportional to E.

Currents were not measured directly. Resistors of 10^{10} and 10^{11} ohms were placed across the input terminals of an Applied Physics Corporation vibrating reed electrometer, model 30. The potential difference between the drop in the high resistor and an adjustable potential from a Rubicon portable precision potentiometer was amplified by the electrometer and observed on a Brown electronic, self-balancing, recording potentiometer. The electrometer and recorder system was thus used only as a null indicator. The potentiometer settings required for each null were recorded and later converted to currents.

The outer sphere potentials were measured in a similar manner. The potentials were divided using a calibrated potential divider and compared to potentials from a Rubicon potentiometer, model 2730. Nulls were observed with a Brown null indicator, model 104WIG. The potentials required for each null were recorded and later converted to the outer sphere potentials.

The potentials applied to the outer sphere were obtained using the following power supplies: a Keithley model 240 (0 - 1000 V), John Fluke Manufacturing Company models 400DBA (0 - 5000 V) and 410A (0 - 10 KV), and a Beta Electric Company model 206 (0 - 30 kV). An additional double L-section filter was used with the Beta supply to reduce ripple. Each section consisted of a 1-megohm resistor and 0.45-microfarad condenser. An additional 15-megohm resistor protected the Keplertron from corona

discharge inside the vacuum tank.

Measurements were made in vacua of about 10^{-6} mm Hg and with Faraday cup biases of 23 V for the disk source and 24.5 V for the cavity source. The cup was at ground potential and a negative potential was applied to the exit slit grid.

Initial dose rates of the operator's chair were about 2 mr/hr for the disk source and 10 mr/hr for the cavity source. In each case the total dose received by the operators was less than 50 mr.

V. DATA ANALYSIS

A. Source Activity

Since the theoretical electron flux was normalized to one electron born per cm^3, it was necessary to determine the absolute disintegration rate for both sources. This was done with a gamma scintillation spectrometer consisting of a Nuclear Data model 101 analyzer with a NaI(Tl) crystal. The photo-peak-to-total count ratios and efficiencies used were those given by Heath.[11] The disk source (excluding the screw) had an activity $(1.27 \pm 0.05) \times 10^{11}$ disintegrations per second and the cavity an activity of $(5.13 \pm 0.15) \times 10^{11}$ disintegrations per second at the time of removal from the reactor. The activities stated have been corrected for absorption of gamma rays in the sources.

B. Corona Discharge

Corona discharge within the Keplertron prevented measurements of the electron flux above 37 keV. The discharge contributed less than 0.1% to the electron flux below 10 keV and less than 2% to the electron flux at 37 keV. A partial disassembly of the Keplertron after data had been taken revealed that a metal screen which formed the part of the outer sphere directly opposite the source had broken loose at the edge, leaving many small wires projecting into the space between the spheres. Fortunately no electron trajectories were interrupted by these wires because of their location. These wires were assumed to be the cause

---

[11] R. L. Heath, U. S. AEC Idaho Operations Office Report IDO-16408, 1957.

of the discharge. All data presented here were corrected by subtracting discharge current measured with no source present.

C. Gamma-Ray Background

Electrons which were ejected in the vicinity of the Faraday cup by gamma rays were attracted to the cup because of the potential difference between the exit slit grid and the Faraday cup. This resulted in a significant current when no potential was applied to the outer sphere. In order to correct for this error, a 150-mc Cs^{137} source was placed on the inner sphere at the source position, and a spectrum was obtained by varying the outer sphere potential. The spectrum thus obtained was normalized to have the same magnitude at zero outer sphere potential as each of the copper spectra. The proper normalized spectrum was then subtracted from each of the copper spectra. Background currents of about 7.5×10^{-14} amp for the disk source and 5.0×10^{-13} amp for the cavity source were observed.

D. Grid Transmission

A correction was also made for the transmission of the grid placed at the exit slit to lower the capacitance between the Faraday cup and the outer sphere. This transmission calculated from the geometrical area of the exit slit obstructed by the grid and supports is 0.96.

E. Keplertron Energy Window Correction

When adjusted to "accept" electrons of energy E_o, the Keplertron actually does not accept electrons with energy E_o exactly but electrons having a finite energy spread. The transmission of electrons as a function of energy is given by Equations (10) through (12) with the added

condition that $T(\delta) = 0$ where not defined by Equations (10) and (11). This instrumental response characteristic may be approximated as rectangular in shape having an energy span ΔE_o equal to the width at half height of the actual response. This width is given by Equation (9) as

$$\Delta E_o = \frac{E_o}{16} \tag{15}$$

for $\chi = 1$.

The height of the transmission profile is determined by the geometry of the source as it relates to the angular acceptance of the Keplertron. For example, for a point isotropic source this height is given by Equation (8) as

$$T = \frac{1}{4} \tag{16}$$

for $\chi = 1$.

For more complicated sources, other calculations are required in order to relate the electron flux within the source to the actual observed Faraday cup current. Such calculations are discussed in Section V, Part F, and are presented in Appendix III in detail for the disk and cavity sources used here. The correction for energy window remains simple for sources of any geometry, however. The observed current is simply attributed to electrons having an energy between E_o and $E_o + \Delta E_o$. Thus, the current per unit energy is obtained by dividing the current by ΔE_o which, according to Equation (15) is just $E_o/16$.

F. Correction for "Probe Area"

The theoretical electron flux is the number of electrons per unit time which would be observed crossing a spherical probe of unit cross-sectional area placed in a medium containing uniformly distributed

radioactivity and integrated over all angles. To obtain an experimental electron flux equivalent to the theoretical flux, the observed electron flux was multiplied by a normalization factor which corrected for the apparent area of the source as seen through the angular acceptance range of the Keplertron. For the disk source this normalization factor was 18.4 and for the cavity source, 8.21. Calculations of these normalization factors are given in Appendix III.

G. Correction for Positron Flux

The observed negatron flux $y(T)_{obs}$ is composed of components due to the primary negatrons, $y(T)_{pri,n}$, secondaries produced by primary negatrons, $y(T)_{sec,n}$, and secondaries produced by primary positrons, $y(T)_{sec,p}$, and is given by

$$y(T)_{obs} = y(T)_{pri,n} + y(T)_{sec,p} + y(T)_{sec,n} \qquad (17)$$

The total flux $y(T)$ without regard to the sign of the charge includes also the contribution due to primary positrons, and is given by

$$y(T) = y(T)_{obs} + y(T)_{pri,p} \qquad (18)$$

In the theoretical electron slowing down calculations, it is assumed that one electron of either sign is born per cm^3. This assumption was made possible by the near identity of the primary negatron and positron spectral shapes for Cu^{64} which is even more pronounced in the integral form in which the spectra enter the calculations. Thus it is desirable to obtain a conversion factor by which to multiply the experimental results in order to compare them with theory, i.e., to infer from the experimental electron flux, the flux which would be observed if the Keplertron could detect the primary positron flux in addition to the

components of Equation (17). This is accomplished in the following manner. In the nuclear decay of Cu^{64} there are two negatron disintegrations for each positron disintegration. If the stopping power for negatrons given by Bethe[12] is assumed to be identical to that for positrons given by Rohrlich and Carlson[13] for the purposes of this calculation (see the discussion of this point by Birkhoff[14]), then

$$y(T)_{pri,p} = \frac{1}{2}\, y(T)_{pri,n}. \tag{19}$$

Furthermore, if the Möller[15] and Bhabha[16] cross sections for the production of secondary electrons from negatrons and positrons respectively are assumed to be the same, then the secondary to primary ratio will be identical also, and is given by

$$\frac{y(T)_{sec,n}}{y(T)_{pri,n}} = \frac{y(T)_{sec,p}}{y(T)_{pri,p}} = \frac{A}{S}. \tag{20}$$

Equations (17) through (20) may be solved to eliminate all fluxes except $y(T)$ and $y(T)_{obs}$ with the result,

$$y(T) = y(T)_{obs} \left[1 + \frac{1}{2(1 + \frac{3}{2}\frac{A}{S})}\right] \tag{21}$$

For comparison with theory, the observed electron fluxes were multiplied by the correction factor in [ ] in Equation (21) where the ratio A/S was taken from the theoretical calculations given in Appendix I. At 37 keV

---

[12] H. A. Bethe, in Handbuch der Physik, edited by H. Geiger and K. Scheel (Verlag Julius Springer, Berlin, 1933), Vol. 24, Part 1, p. 273.

[13] F. Rohrlich and B. C. Carlson, Phys. Rev. 93, 38 (1954).

[14] R. D. Birkhoff, loc. cit.

[15] C. Möller, Ann. Physik 14, 531 (1932).

[16] H. J. Bhabha, Proc. Roy. Soc. (London) A154, 195 (1936).

the correction increased the observed electron flux by 39% and below 100 eV by less than 1%. At the higher energy the correction depends primarily upon the relative number of positrons and negatrons in the nuclear decay and not upon the theoretical ratio A/S. Although at the lower energy the dependence upon A/S is greater and the correction is less certain, the correction is much smaller.

VI. RESULTS

Figures 12 and 13 show the calculated electron flux spectrum and the results obtained from the disk source and cavity source, respectively. The curves are not fitted and neither the theoretical calculations nor the experimental corrections contain adjustable parameters. The contributions of the primary and secondary electrons to the theoretical electron flux are also shown. Calculations were stopped at 30 eV because of the lack of experimental or theoretical values of stopping power. As expected, the disk flux approaches the theoretical cavity flux at high energies but is lower in the region near 10 keV because the disk is a semi-infinite medium, not an infinite medium as assumed in the theory. The large rise at lower energies and the peak at 3 eV are due to secondary electrons but corrections may be required for scattering off the Keplertron spheres. The smaller peak at 7 keV is composed of two unresolved peaks; the Cu^{64} KLL Auger line which is initiated by an energetic electron colliding with and ejecting a K-electron from a Cu atom and Ni^{64} KLL Auger line which is initiated by electron capture in the nuclear decay of Cu^{64}.

The experimental flux from the cavity source, corrected for instrument response as described in Section V, is in good agreement from 37 keV to 1 keV with the theory. Below 1 keV the experimental spectrum is uncertain due to scattering off the spheres, and the theory is questionable since the Möller formula assumes unbound electrons, and this is certainly not true at energies less than the energy of the L-shell. It is worth noting that the low energy peak is higher for the

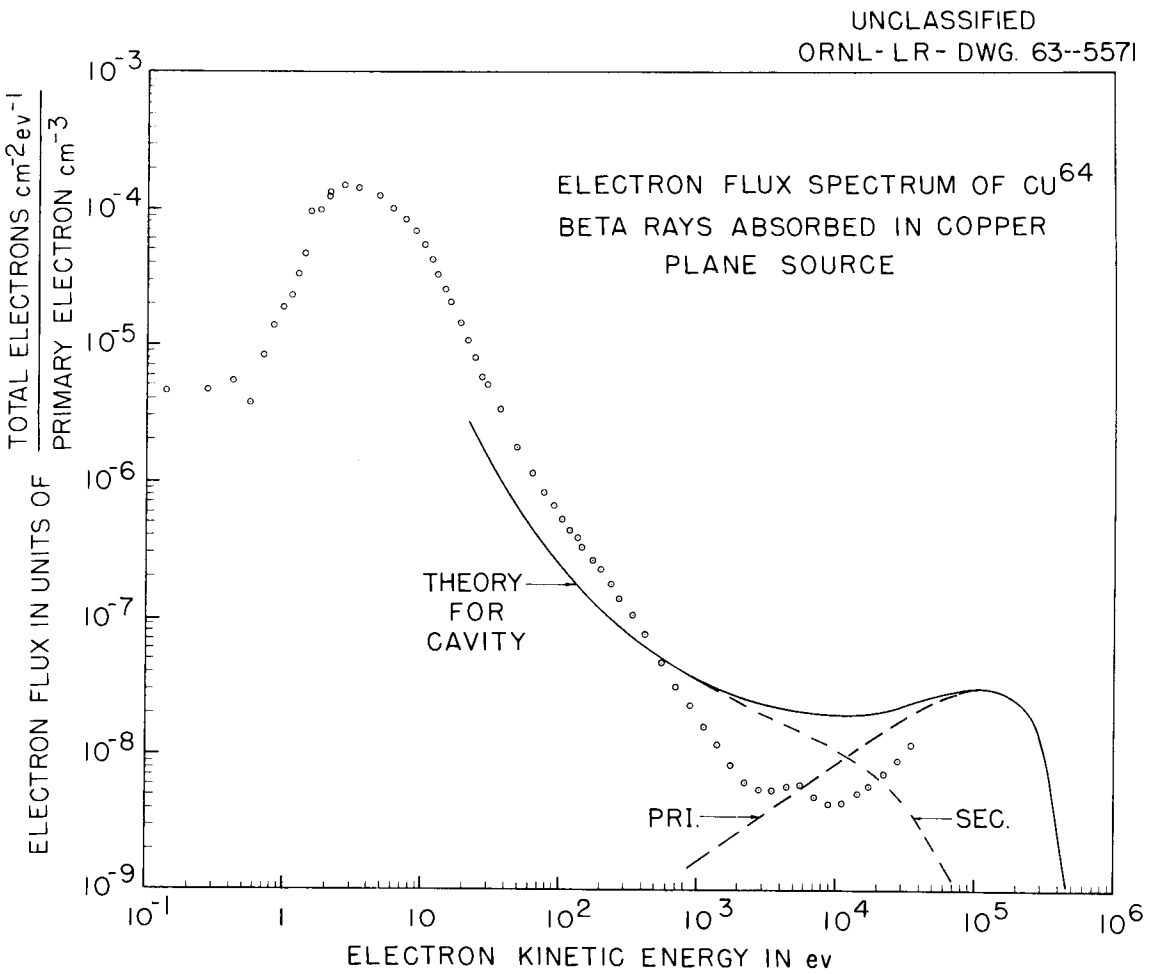

Fig. 12. Electron Flux Spectrum of Cu^{64} Beta Rays Absorbed in Copper Plane Source.

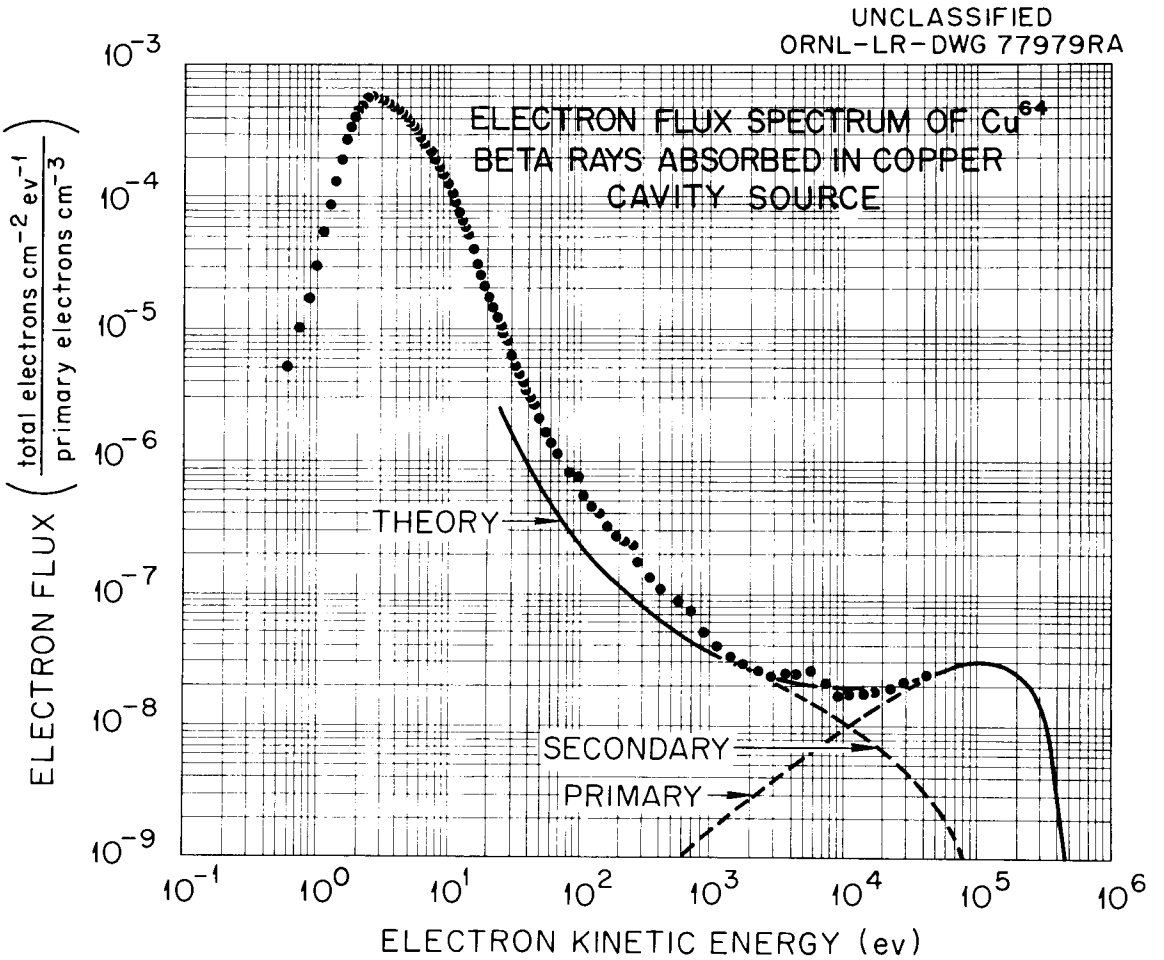

Fig. 13. Electron Flux Spectrum of Cu^{64} Beta Rays Absorbed in Copper Cavity Source.

cavity than for the disk. However, this needs further study and verification.

VII. CONCLUSIONS

The Keplertron, a spherical, electrostatic focusing, beta spectrometer, was calibrated from 1 eV to 3 keV using an electron gun which approximated a point source and at 31.4 keV using th Sm^{152} KLL Auger line from a Eu-152 source of thickness 50 $\mu g/cm^2$. The electron gun measurements agreed with the theoretical values of 6.3% for the energy resolution and 25% for the transmission. Deviations from theory at low energies were observed but were attributed to the energy spread of electrons from the electron gun. The Eu^{152} source gave values of $(7 \pm 1)\%$ for the energy resolution and $(25 \pm 7)\%$ for the transmission. The energy of the electrons transmitted for both sources was 1.37 times the outer sphere potential as compared with the theoretical value of 1.50. The reasons for this difference have not been determined. Line profiles agree well with theory.

The electron flux spectrum resulting from the slowing down of electrons from Cu^{64} uniformly distributed in Cu was measured from 37 keV to 0.1 eV for both a plane disk source and a "black body cavity" source using the Keplertron. These measurements showed that the electron flux spectrum for the cavity corrected for instrumental response as described in Section V is in good agreement from 37 keV to 1 keV with the simplified Spencer-Fano theory. Although further study is required on scattering off the Keplertron spheres in the region below 1 keV, these measurements suggest that in material irradiated by high energy electrons, there is a buildup of several orders of magnitude in the electron flux below 1 keV compared to the electron flux at 10 keV.

APPENDIX I

SAMPLE CALCULATION OF ELECTRON FLUX

The calculation of the electron flux spectrum is made according to the Spencer-Fano-Attix theory as outlined in Section 1. A calculation for copper containing Cu^{64} is given here.

Equation (7) of Section 1 may be written

$$y(T) = \left[S_Z(T)\right]^{-1} \left\{S(T) + \int_{2T}^{T_o} dT' H(T') \left[\frac{1}{T} + \frac{1}{T - T'}\right] y(T')\right\} \tag{22}$$

where $y(T)$ is the electron flux in units of $(\text{eV cm}^2 \text{ sec})^{-1}$, $S_Z(T)$ in units of eV cm^{-1} is the stopping power of the absorbing material of atomic number Z for electrons of energy T, and $H(T')$ in units of eV cm^{-1} is defined as

$$H(T') = 2\pi m_o c^2 N_o r_o^2 \rho (Z/A)(\beta')^2 \tag{23}$$

where $m_o c^2$ is the electron rest energy in eV; N_o is Avogadro's number: r_o is the classical electron radius in cm; ρ, Z, and A are the density, atomic number, and atomic weight, respectively, of the absorbing material; and $\beta' = v'/c$ measures the velocity of the electron. The function $S(T)$ is the integrated source spectrum and is defined by

$$S(T) = \int_T^{T_o} N(T') dT' \tag{24}$$

where $N(T')$ is the primary beta spectrum in units of $(\text{eV cm}^3 \text{ sec})^{-1}$. The quantity

$$H(T) \left[\frac{1}{T} + \frac{1}{T - T'}\right] \tag{25}$$

with energies in eV is an approximation of the integrated Möller cross section.[17] By defining a function

$$R(T) = H(T)\ y(T) \tag{26}$$

and expressing the stopping power as

$$S_Z(T) = H(T)\ B(T) \tag{27}$$

where B(T) is a pure number often called the "stopping number", Equation (22) may be rewritten as

$$R(T) = \left[B(T)\right]^{-1} \left\{S(T) + \int_{2T}^{T_o} \left[\frac{T'}{T} + \frac{T'}{T - T'} \right] R(T')\ \frac{dT'}{T'} \right\} \tag{28}$$

where the integrand has been multiplied and divided by T' in order to illustrate the utility of introducing a logarithmic energy parameter. A set of points T_i must be chosen at which the integrand is to be evaluated. For the purpose of this calculation it was convenient to distribute the T_i evenly on a scale of lnT, i.e., T_o, ξT_o, $\xi^2 T_o$, etc. The ξ used here was chosen such that $\xi^3 = 1/2$, or $\xi^n = (1/2)^{n/3}$.

The problem may now be further simplified by introducing the logarithmic energy intervals into Equation (28). Let $\mu = \ln(T_o/T)$; then $T = T_o e^{-\mu}$ and $T' = T_o e^{-\mu'}$. It follows that $d\mu' = dT'/T'$ and

$$(\mu')_{T'=2T} = \left(\ln\frac{T_o}{T'}\right)_{T'=2T} = \ln\frac{T_o}{2T} = \mu - \ln 2$$

and

$$(\mu)_{T'=T_o} = \left(\ln\frac{T_o}{T'}\right)_{T'=T_o} = \ln\frac{T_o}{T_o} = 0,$$

---

[17] Birkhoff, Hubbell, Cheka, and Ritchie, loc. cit.

so

$$R(T_o,\mu) = \left[B(T_o,\mu)\right]^{-1} \left\{S(T_o,\mu) + \int_0^{\mu-\ln 2} \left[e^{(\mu-\mu')} + (e^{-(\mu-\mu')} - 1)^{-1}\right] R(T_o,\mu')d\mu'\right\} \tag{29}$$

Equation (29) is a Volterra type integral equation and the usual method of solution is to approximate the integral by finite sums. Using this method, Equation (29) becomes

$$R_n = B_n^{-1} \left\{S_n + \sum_{m=0}^{m=n-3} \left[e^{(n-m)\Delta\mu} + (e^{-(n-m)\Delta\mu} - 1)^{-1}\right] C_m R_m\right\} \tag{30}$$

The quantity $\left[e^{(n-m)\Delta\mu} + (e^{-(n-m)\Delta\mu} - 1)^{-1}\right]$ is designated as K_{n-m} in what follows. Because m is always less than n, R_m of Equation (30) is one of the values of R_n previously calculated. The quantity C_m is a weight factor determined from Simpson's rule and Cote's rule.

Simpson's rule, may be written as

$$\int_c^d y(x)dx \cong [h/3][y_o + y_b + 4(y_1 + y_3 + \ldots + y_{b-1}) + 2(y_2 + y_4 + \ldots +_{b-2})]$$

$$b = 2a;\ a = 1, 2, 3\ldots \tag{31}$$

Cote's rule or the 3/8 rule, may be written as

$$\int_c^d y(x)dx \cong [3h/8][y_o + 3y_1 + 3y_2 + y_3]. \tag{32}$$

The $\int_c^d y(x)dx$ is the area under the curve between c and d, and h is the distance between successive ordinates of the subdivision used in approximately the integral. In this case $h = \Delta\mu = (1/3)(\ln 2.)$ Simpson's rule is used for odd n and for even n where m is greater than three. Cote's rule is used for even n where m = 0, 1, 2, 3. Pictorially

this might be represented as follows:

$$m = \overbrace{0\ 1\ 2}^{S}$$

$$m = \overbrace{0\ 1\ 2\ 3}^{C}$$

$$m = \overbrace{0\ 1\ 2}^{S}\overbrace{\ 3\ 4}^{S}$$

$$m = \overbrace{0\ 1\ 2\ 3}^{C}\overbrace{\ 4\ 5}^{S}$$

$$m = \overbrace{0\ 1\ 2}^{S}\overbrace{\ 3\ 4}^{S}\overbrace{\ 5\ 6}^{S}$$

$$m = \overbrace{0\ 1\ 2\ 3}^{C}\overbrace{\ 4\ 5}^{S}\overbrace{\ 6\ 7}^{S}$$

etc.

From Equations 31 and/or 32 and the equation

$$R_n = B_n^{-1}\left\{S_n + \sum_{m=0}^{m=n-3} K_{n-m}\, C_m R_m\right\} \tag{33}$$

$$K_{n-m} = 0 \text{ for } n-m = 1,2,3,$$

the C_m may be evaluated for the case $h = (1/3)(\ln 2)$ as follows:

$m = 5$ $(n=8)$

$$\int_c^d y(x)\,dx = (1/8)(\ln 2)[y_o + 3y_1 + 3y_2 + y_3] + (1/9)(\ln 2)\ [(y_3 + y_5) + 4y_4]$$

$$= (1/8)(\ln 2)\ y_o + (3/8)(\ln 2)y_1 + (3/8)(\ln 2)y_2$$

$$+ (17/72)(\ln 2)y_3 + (4/9)(\ln 2)y_4 + (1/9)(\ln 2)y_5.$$

In general form, the C_m are:

even n	odd n
$C_o = (1/8)(\ln 2)$	$C_o = (1/9)(\ln 2)$
$C_1 = (3/8)(\ln 2)$	$C_1 = (4/9)(\ln 2)$
$C_2 = (3/8)(\ln 2)$	$C_2 = (2/9)(\ln 2)$
$C_3 = (17/72)(\ln 2)$	$C_3 = (4/9)(\ln 2)$
$C_4 = (4/9)(\ln 2)$	$C_4 = (2/9)(\ln 2)$
$C_5 = (2/9)(\ln 2)$	.
$C_6 = (4/9)(\ln 2)$	.
$C_7 = (2/9)(\ln 2)$	.
.	$C_{n-5} = (2/9)(\ln 2)$
.	$C_{n-4} = (4/9)(\ln 2)$
.	$C_{n-3} = (1/9)(\ln 2)$
$C_{n-5} = (2/9)(\ln 2)$	
$C_{n-4} = (4/9)(\ln 2)$	
$C_{n-3} = (1/9)(\ln 2)$	

The caluclation is begun from a knowlege of R_o through R_4. Since $S_o = 0$, then $R_o = 0$. Since $K_{n-m} = 0$ for m = 1, 2, 3, and $K_4 (= 0.8619)$ is multiplied by $R_o = 0$, then $R_1 = B_1^{-1} S_1$, $R_2 = B_2^{-1} S_2$, $R_3 = B_3^{-1} S_3$, and $R_4 = B_4^{-1} S_4$. Using these values, R_5, R_6, R_7, and R_8 may be obtained.

From Equation 33,

$$R_5 = B_5^{-1} \left\{ S_5 + \sum_{m=0}^{m=2} K_{5-m} C_m R_m \right\}$$

or

$$R_5 = B_5^{-1} \left\{ S_5 + \left[C_o R_o K_5 + C_1 R_1 K_4 + C_2 R_2 K_3 \right] \right\}$$

and by the same method,

$$R_6 = B_6^{-1} \left\{ S_6 + \left[C_o R_o K_6 + C_1 R_1 K_5 + C_2 R_2 K_4 + C_3 R_3 K_3 \right] \right\}$$

$$R_7 = B_7^{-1} \left\{ S_7 + \left[C_o R_o K_7 + C_1 R_1 K_6 + C_2 R_2 K_5 + C_3 R_3 K_4 + C_4 R_4 K_3 \right] \right\}$$

$$R_8 = B_8^{-1} \left\{ S_8 + \left[C_o R_o K_8 + C_1 R_1 K_7 + C_2 R_2 K_6 + C_3 R_3 K_5 + C_4 R_4 K_4 + C_5 R_5 K_3 \right] \right\}.$$

These may now be used to obtain R_9, R_{10}, R_{11}, and R_{12}. Denoting the quantity in brackets, $[\ ]$, as A_n, Equation 30 may be written

$$R_n = B_n^{-1} \left\{ S_n + A_n \right\} \tag{34}$$

where S_n represents the source of primary electrons, and A_n represents the additional source of secondary electrons.

A tabulation of the calculation is given in Table 2. The stopping power used from 571 keV to 10 keV was taken from the supplement to NBS Circular 577.[18] From 10 keV to 5.5 keV the Bethe-Bloch formula fitted smoothly with the NBS values. Below 5.5 keV the experimental proton stopping power for copper[19] was used, assuming that protons and electrons

---

[18] A. T. Nelms, Supplement to National Bureau of Standards Circular No. 577, 1958.

[19] W. Whaling, in Handbuch der Physik, edited by S. Flügge (Springer-Verlag, Berlin, 1958), Vol. 34, p. 202.

of the same velocity slow down in the same manner. The lowest energy at which the proton stopping power was used was 50 keV. At this energy the ratio[20] of charged to uncharged hydrogen atoms is 2:1 and this number increases rapidly as the proton energy increases. Because the uncertainty introduced by the proton charge is smaller than other uncertainties at low energy (i.e. the applicability of the theory itself), the proton stopping power was not corrected for electron capture and loss. The electron stopping power obtained from that for protons was normalized to fit the Bethe-Bloch stopping power at 5.5 keV by multiplying by 0.75. Figure 14 shows the electron stopping power as a function of energy.

---

[20] C. F. Barnett, W. B. Gauster, and J. A. Ray, Oak Ridge National Laboratory Report, ORNL-3113, 1961.

TABLE 2 - a

CALCULATION OF ELECTRON FLUX IN COPPER CONTAINING Cu^{64}

n - m or n	$\xi = (1/2)^{m/3}$	Electron Energy $T = \xi T_o$ $T_o = 5.71 \times 10^5$	β^2	H_n^{-1}	Stopping Power $(S_z)_n$	Stopping Number B_n	B_n^{-1}
		(eV)		$(\frac{eV}{cm})^{-1}$	$(\frac{eV}{cm})$		
0	1.00	5.71×10^5	7.74×10^{-1}	1.23×10^{-6}	1.19×10^7	1.47×10	6.80×10^{-2}
1	9.94×10^{-1}	4.53	7.23	1.15	1.25	1.44	6.94
2	6.30	3.60	6.56	1.05	1.30	1.36	7.35
3	5.00	2.86	5.93	9.60×10^{-7}	1.40	1.34	7.62
4	3.97	2.27	5.18	8.27	1.55	1.28	7.46
5	3.15	1.80	4.62	7.37	1.70	1.25	8.00
6	2.50	1.43	3.97	6.33	1.90	1.20	8.33
7	1.98	1.13	3.36	5.33	2.20	1.17	8.54
8	1.57	8.99×10^4	2.81	4.47	2.50	1.11	9.01
9	1.25	7.14	2.30	3.67	2.90	1.06	9.43
10	9.92×10^{-2}	5.67	1.94	3.10	3.35	1.04	9.62
11	7.87	4.50	1.56	2.49	3.90	9.69×10^0	1.03×10^{-1}
12	6.25	3.57	1.26	2.00	4.60	9.18	1.09
13	4.96	2.83	1.01	1.61	5.40	8.69	1.15
14	3.94	2.25	8.12×10^{-2}	1.30	6.30	8.14	1.23
15	3.13	1.78	6.50	1.04	7.50	7.78	1.29
16	2.48	1.42	5.29	8.45×10^{-8}	8.80	7.41	1.35
17	1.97	1.12	4.12	6.55	1.05×10^8	6.85	1.46
18	1.56	8.92×10^3	3.31	5.29	1.23	6.51	1.54
19	1.24	7.08	2.62	4.17	1.50	6.26	1.60
20	9.82×10^{-3}	5.61	2.16	3.45	1.75	6.02	1.66
21	7.82	4.47	1.69	2.69	2.10	5.63	1.78
22	6.20	3.54	1.37	2.18	2.47	5.36	1.87
23	4.92	2.81	1.06	1.69	2.90	4.90	2.04

Table 2 - a continued

n - m or n	$\xi = (1/2)^{m/3}$	Electron Energy $T = \xi T_o$ $T_o = 5.71 \times 10^5$	β^2	H_n^{-1}	Stopping Power $(S_z)_n$	Stopping Number B_n	B_n^{-1}
		(eV)		$(\frac{eV}{cm})^{-1}$	$(\frac{eV}{cm})$		
24	3.91×10^{-3}	2.23×10^3	8.46×10^{-3}	1.35×10^{-8}	3.45×10^8	4.66×10^0	2.15×10^{-1}
25	3.10	1.77	6.72	1.07	4.10	4.38	2.28
26	2.46	1.40	5.48	8.74×10^{-9}	4.80	4.19	2.39
27	1.95	1.11	4.36	6.96	5.60	3.91	2.56
28	1.55	8.85×10^2	3.36	5.33	6.00	3.18	3.14
29	1.23	7.02	2.70	4.31	7.20	3.10	3.23
30	9.76×10^{-4}	5.57	2.16	3.45	8.30	2.85	3.50
31	7.76	4.43	1.72	2.74	9.20	2.52	3.97
32	6.16	3.52	1.37	2.18	1.03×10^9	2.24	4.47
33	4.88	2.79	1.09	1.73	1.12	1.94	5.16
34	3.88	2.22	8.41×10^{-4}	1.34	1.21	1.62	6.18
35	3.08	1.76	6.76	1.08	1.31	1.41	7.09
36	2.45	1.40	5.29	8.45×10^{-10}	1.40	1.18	8.48
37	1.94	1.11	4.20	6.68	1.49	9.96×10^{-1}	1.00×10^0
38	1.54	8.79×10	3.42	5.47	1.52	8.29	1.21
39	1.22	6.97	2.72	4.33	1.55	6.70	1.49
40	9.70×10^{-5}	5.54	2.16	3.45	1.53	5.26	1.90
41	7.70	4.40	1.69	2.69	1.49	4.00	2.50
42	6.11	3.49	1.35	2.16	1.42	3.06	3.27
43	4.85	2.77	1.08	1.72	1.35	2.32	4.31

TABLE 2 - b

CALCULATION OF ELECTRON FLUX IN COPPER CONTAINING CU^{64}

n - m or n	Integrated Source S_n Spectrum	K_{n-m}	$S_n + A_n$	R_n	Total Electron Flux $(Y_n)_t$	Primary Electron Flux $(Y_n)_S$	Secondary Electron Flux $(Y_n)_A$
	$(cm^3 sec)^{-1}$		$(cm^3 sec)^{-1}$	$(cm^3 sec)^{-1}$	$(eV\ cm^2 sec)^{-1}$	$(eV\ cm^2 sec)^{-1}$	$(eV\ cm^2 sec)^{-1}$
0	0.000	0.00	0.00	0.00	0.00	0.00	0.00
1	0.022	0.00	2.20×10^{-2}	1.53×10^{-3}	1.76×10^{-9}	1.76×10^{-9}	0.00
2	0.105	0.00	1.05×10^{-1}	7.72	8.08	8.08	0.00
3	0.225	0.00	2.25	1.68×10^{-2}	1.61×10^{-8}	1.61×10^{-8}	0.00
4	0.350	8.62×10^{-1}	3.50	2.67	2.26	2.26	0.00
5	0.470	1.72×10^{0}	4.70	3.76	2.76	2.76	0.00
6	0.572	2.67	5.74	4.78	3.01	3.01	0.00
7	0.658	3.79	6.66	5.69	3.03	2.99	4.00×10^{-10}
8	0.730	5.16	7.49	6.75	3.01	2.92	9.00
9	0.785	6.86	8.23	7.76	2.84	2.71	1.30×10^{-9}
10	0.830	8.97	8.98	8.64	2.68	2.48	2.00
11	0.869	1.16×10	9.82	1.01×10^{-1}	2.50	2.23	2.70
12	0.900	1.49	1.08×10^{0}	1.18	2.35	1.96	3.90
13	0.920	1.91	1.19	1.37	2.19	1.70	4.90
14	0.940	2.44	1.33	1.64	2.13	1.49	6.40
15	0.950	3.10	1.51	1.95	2.02	1.27	7.50
16	0.960	3.92	1.74	2.35	1.98	1.09	8.90
17	0.972	4.95	2.04	2.98	1.95	9.26×10^{-9}	1.02×10^{-8}
18	0.975	6.30	2.43	3.74	1.98	7.93	1.19
19	0.980	8.25	2.95	4.72	1.98	6.53	1.33
20	0.985	1.04×10^{2}	3.62	6.01	1.98	5.63	1.42
21	0.987	1.30	4.50	8.01	2.15	4.70	1.68
22	0.990	1.62	5.66	1.06×10^{0}	2.31	4.01	1.91
23	0.992	2.05	7.18	1.46	2.47	3.42	2.13

Table 2 - b continued

n - m or n	Integrated Source S_n Spectrum	K_{n-m}	$S_n + A_n$	R_n	Total Electron Flux $(Y_n)_t$	Primary Electron Flux $(Y_n)_S$	Seconday Electron Flux $(Y_n)_A$
	$(cm^3 sec)^{-1}$		$(cm^3 sec)^{-1}$	$(cm^3 sec)^{-1}$	$(eV\ cm^2 sec)^{-1}$	$(eV\ cm^2 sec)^{-1}$	$(eV\ cm^2 sec)^{-1}$
24	0.995	2.58×10^2	9.18×10^0	1.97×10^0	2.66×10^{-8}	2.88×10^{-9}	2.37×10^{-8}
25	0.998	3.26	1.18×10	2.69	2.88	2.43	2.64
26	0.999	4.13	1.52	3.63	3.17	2.08	2.96
27	1.000	5.14	1.97	5.04	3.50	1.79	3.32
28	1.000	6.53	2.56	8.04	4.29	1.67	4.12
29	1.000	8.22	3.34	1.08×10	4.66	1.39	4.52
30	1.000	1.03×10^3	4.37	1.53	5.26	1.20	5.14
31	1.000	1.31	5.74	2.28	6.24	1.09	6.13
32	1.000	1.64	7.60	3.22	7.34	9.62×10^{-10}	7.24
33	1.000	2.08	1.00×10^2	5.16	8.92	8.92	8.83
34	1.000	2.67	1.34	8.28	1.11×10^{-7}	8.26	1.03×10^{-7}
35	1.000	3.30	1.78	1.26×10^2	1.36	7.63	1.28
36	1.000	4.11	2.38	2.02	1.70	7.14	1.63
37	1.000	5.22	3.24	3.24	2.15	6.72	2.08
38	1.000	6.64	4.43	5.36	2.94	6.58	2.88
39	1.000	8.27	6.11	9.10	3.93	6.45	3.87
40	1.000	1.05×10^4	8.40	1.60×10^3	5.52	6.54	5.46
41	1.000	1.04	1.98×10^3	4.95	1.33×10^{-6}	6.72	1.26×10^{-6}
42	1.000	1.66	1.73	5.66	1.22	7.04	1.15
43	1.000	2.07	2.53	1.09×10^4	1.87	7.36	1.80

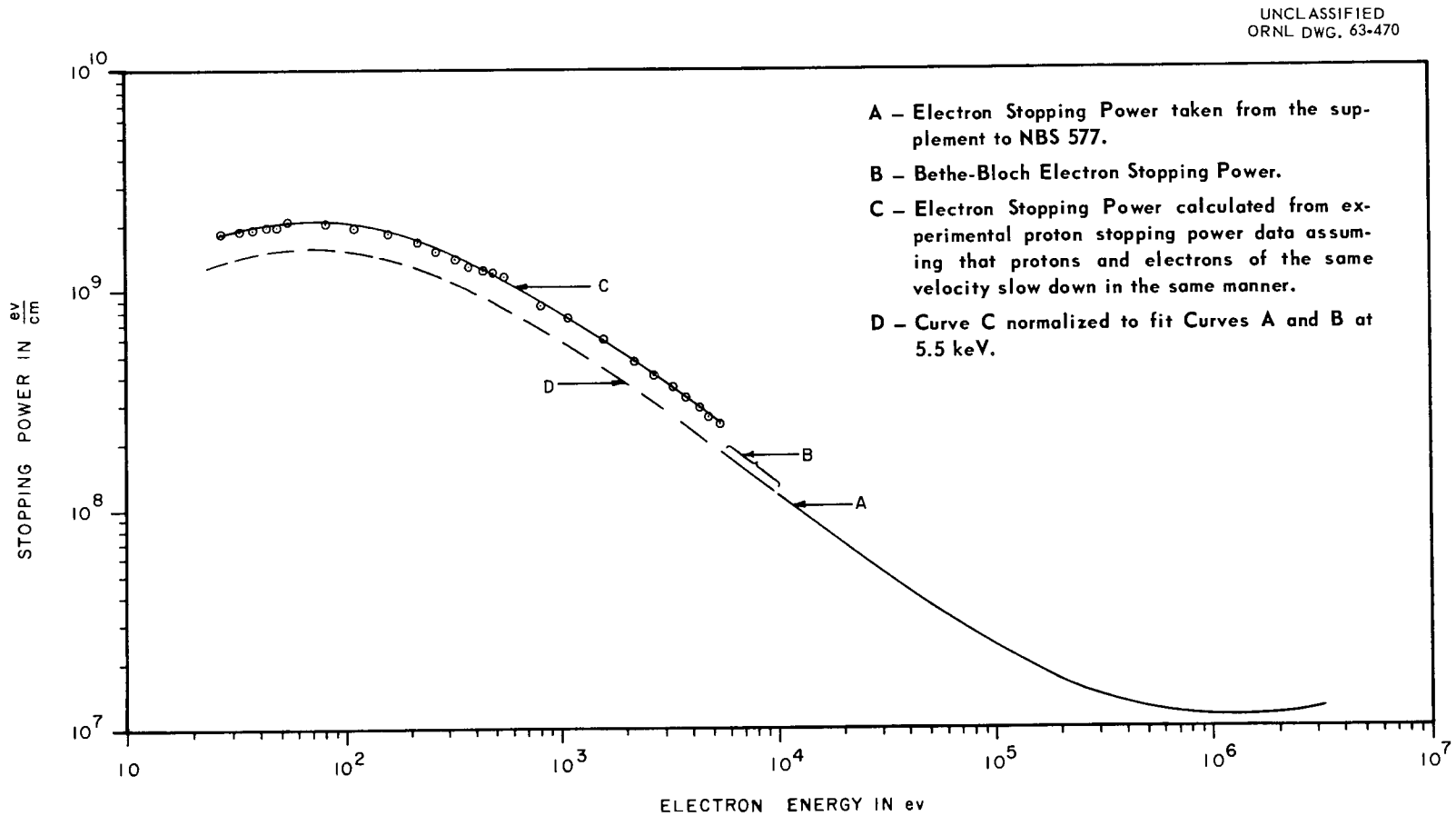

Fig. 14. Electron Stopping Power for Copper.

APPENDIX II

SOLID ANGLE SUBTENDED AT ONE HOLE BY THE REMAINING OPEN AREA OF THE CAVITY SOURCE

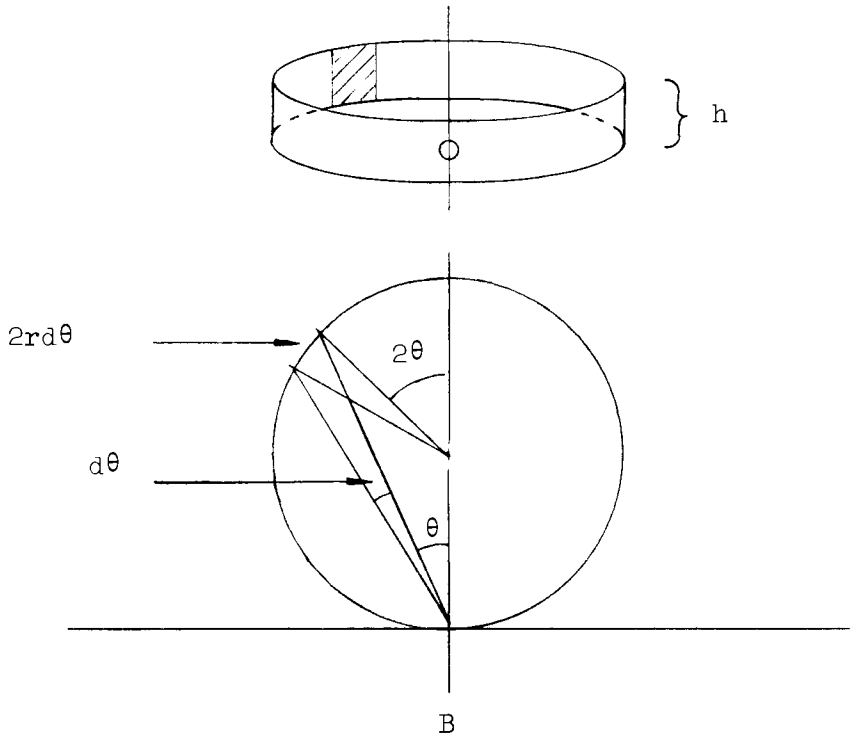

Assume the source to be a cylinder h units in height, where $h < 2r$, and the hole under consideration to be at point B, a distance of h/2 above the base. The differential solid angle subtended at B by the open area of the curved surface of the cylinder is approximately

$$d\Omega = \frac{1}{2} \frac{2\ hr \cos\theta\ d\theta}{(2r \cos\theta)^2} \tag{35}$$

where the factor 1/2 is introduced because the surface is 50% open. The total solid angle subtended at B by the open area of the curved surface of the cylinder is

$$\Omega = \frac{h}{2r} \log \tan \left(\frac{\pi}{4} + \frac{\Phi}{2}\right) \tag{36}$$

where Φ is the angle at which no effective open area remains. For the source used here $\Phi = 80^{\circ}$ and $h \approx r$. Thus, $\Omega \approx 1$ steradian and the fractional solid angle subtended at B is approximately $1/(2\pi) = 0.16$. Thus, for each hole the source appears to be about 92% solid and only 8% open.

APENDIX III

FLUX NORMALIZATION FACTOR

A. Disk Source

The theoretical electron flux is that which would be observed crossing a spherical probe of unit cross sectional area and integrated over all angles. For comparison with theory, the observed current I must be divided by the apparent area of the disk as seen through the angular acceptance range of the Keplertron. The effective product of source area and solid angle is denoted $(A\Delta\Omega)_{eff}$. If A_d is the area of the disk and θ is the angle measured from the normal to the surface of the disk, then the product of the projected area and the solid angle subtended by the Faraday cup at the source is

$$(A\Delta\Omega)_{eff} = A_d \int_{61.4^\circ}^{90^\circ} 2\pi \sin\theta \cos\theta \, d\theta \tag{37}$$

where the limits on θ are determined by the 28.6° angular acceptance range of the Keplertron and $A_d = 0.946$ cm^2. Thus,

$$(A\Delta\Omega)_{eff} = 0.684 \text{ cm}^2 \text{ steradians.}$$

The current per cm^2 of source and per steradian is $I/(A\Delta\Omega)_{eff}$. For a total solid angle of 4π steradians, the total current per cm^2 or the flux is

$$y = \frac{4\pi \, I}{(A\Delta\Omega)_{eff}} = 18.4 \, I. \tag{38}$$

B. Cavity Source

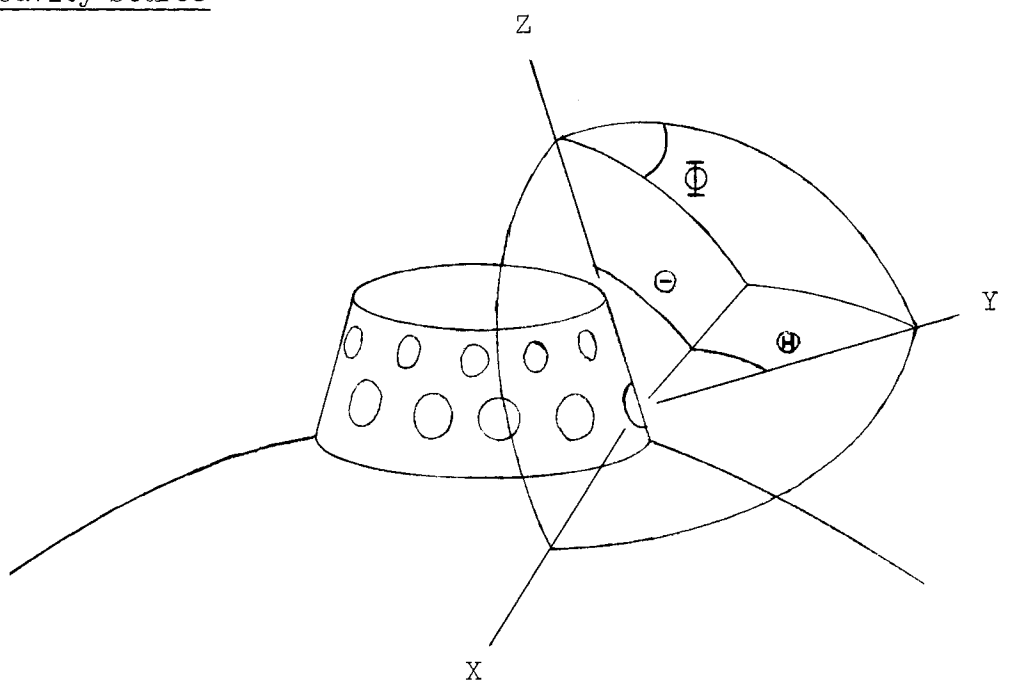

The effective product of source area and solid angle for the cavity source is

$$(A\Delta\Omega)_{eff} = A_c \int_{\Phi_1}^{\Phi_2} d\Phi \int_{\theta_1}^{\theta_2} \cos \Theta \sin \theta \, d\theta \qquad (39)$$

where A_c is the total area of the holes in the source, and $\cos \Theta$ as given for the side of a spherical triangle is

$$\cos \Theta = \cos \theta \cos \pi/2 + \sin \theta \sin \pi/2 \cos \Phi.$$

For the cavity source, $A_c = 1.59 \text{ cm}^2$ and Φ runs from 80° to -80°. The angle θ is governed by the acceptance angle of the Keplertron and runs from 75.7° to 104.3°. If one substitutes these values and the expression for $\cos \Theta$ into Equation (39), then

$$(A\Delta\Omega)_{eff} = 1.53 \text{ cm}^2 \text{ steradians}$$

and

$$y = \frac{4\pi \, I}{(A\Delta\Omega)_{eff}} = 8.21 \, I. \qquad (40)$$

BIBLIOGRAPHY

Barnett, C. F., Gauster, W. B., and Ray, J.A., Atomic and Molecular Collision Cross Sections Interest in Controlled Thermonuclear Research, ORNL-3113 (Oak Ridge National Laboratory, Oak Ridge, Tennessee, 1961)

Bethe, H. A., "Quantenmechanik der Ein-und Zwei - Electronenprobleme," in Handbuch der Physik, edited by H. Geiger and K. Scheel (Verlag Julius Springer, Berlin, 1933), Vol. 24, Part 1, pp. 273-560.

Birkhoff, R. D., "The Passage of Fast Electrons Through Matter," in Handbuch der Physik, edited by S. Flügge (Springer-Verlag, Berlin, 1958), Vol. 34, pp. 121-124.

Birkhoff, R. D., Hubbell, H. H., Jr., Cheka, J. S., and Ritchie, R. H., "Spectral Distribution of Electron Flux in a Beta-Radioactive Medium," Health Phys. 1, 27-33 (1958).

Birkhoff, R. D., Kohn, J. M., Eldridge, H.B., and Ritchie, R. H., "The Spherical Condenser as a High Transmission Particle Spectrometer--Part II. Disk Source," Nuclear Instr. and Methods 8, 313-319 (1960).

Birkhoff, R. D., and Wilkie, W. H., "Measurement of Spectral Distribution of Positron Flux in an Infinite Medium Containing Cu^{64}," Bull. Am. Phys. Soc. 8, 391 (1963).

Bhabha, H. J., "The Scattering of Positrons by Electrons with Exchange on Dirac's Theory of the Positron," Proc. Roy. Soc. (London) A154, 195-206 (1936).

Heath, R. L., Scintillation Spectroscopy Gamma-Ray Spectrum Catalogue, IDO-16408 (Idaho Operations Office, U. S. Atomic Energy Commission, Idaho Falls, Idaho, 1957).

McGinnies, R. T., Energy Spectrum Resulting From Electron Slowing Down, National Bureau of Standards Circular 597 (U.S. Government Printing Office, Washington, D. C., 1959).

Möller, C., "Zur Theorie des Durchgangs schneller Electronen durch Materie," Ann. Physik 14, 531-585 (1932).

Nelms, A. T., Energy Loss and Range of Electrons and Positrons, Supplement to National Bureau of Standards Circular 577 (U.S. Government Printing Office, Washington, D. C., 1958).

Ritchie, R. H., Cheka, J. S., and Birkhoff, R. D., "The Spherical Condenser as a High Transmission Particle Spectrometer--Part I. Point Source," Nuclear Instr. and Methods 6, 157-163 (1960).

Rohrlich, R., and Carlson, B. C., "Positron-Electron Differences in Energy Loss and Multiple Scattering," Phys. Rev. 93, 38-44 (1954).

Spencer, L. V. and Fano, U., "Energy Spectrum Resulting from Electron Slowing Down," Phys. Rev. 93, 1172-1181 (1954).

Spencer, L. V., and Attix, F. H., "A Theory of Cavity Ionization," Rad. Res. 3, 239-254 (1955).

Whaling, W., "The Energy Loss of Charged Particles in Matter," in Handbuch der Physik, edited by S. Flügge (Springer-Verlag, Berlin, 1958), Vol. 34, pp. 193-215.

ORNL-3463
UC-34 — Physics
TID-4500 (29th ed.)

INTERNAL DISTRIBUTION

1. Biology Library
2-4. Central Research Library
5. Reactor Division Library
6-7. ORNL — Y-12 Technical Library
Document Reference Section
8-62. Laboratory Records Department
63. Laboratory Records, ORNL R.C.
64. E. T. Arakawa
65-89. R. D. Birkhoff
90. T. A. Butler
91. L. C. Emerson
92. B. R. Fish
93-112. H. H. Hubbell
113. G. S. Hurst
114. W. H. Jordan
115. R. H. Lafferty, Jr.
116. C. E. Larson
117-141. W. J. McConnell
142. K. Z. Morgan
143. M. J. Skinner
144. J. A. Swartout
145. J. H. Thorngate
146. A. M. Weinberg
147. G. M. Fair (consultant)
148. J. C. Frye (consultant)
149. W. H. Langham (consultant)
150. E. P. Odum (consultant)
151. R. L. Platzman (consultant)
152. L. S. Taylor (consultant)

EXTERNAL DISTRIBUTION

153. Lewis V. Spencer, Physics Department, Ottawa University, Ottawa, Kansas
154. Martin J. Berger, National Bureau of Standards, Washington, D.C.
155. John Laughlin, Memorial Sloan, Kettering Cancer Center, 410 East 68th Street, Department of Physics, New York, New York
156. Werner Brandt, Department of Physics, New York University, New York, New York
157. P. R. J. Burch, Department of Medical Physics, University of Leeds, The General Infirmary, Leeds, England
158. J. B. Birks, University of Manchester, Manchester, England
159. L. G. Augenstein, Biology Research Center, Michigan State University, East Lansing, Michigan
160. K. Seigbohn, University of Uppsala, Uppsala, Sweden
161. K. M. Bisgaard, Institute of Physics, University of Aarhus, Aarhus, Denmark
162. U. Fano, National Bureau of Standards, Washington, D.C.
163. F. H. Attix, National Bureau of Standards, Washington, D.C.
164. J. H. Hamilton, Physics Department, Vanderbilt University, Nashville, Tennessee
165. R. G. Albridge, Physics Department, Vanderbilt University, Nashville, Tennessee
166. D. V. Cormack, University of Saskatchewan, Saskatoon, Canada
167. D. O. Schneider, University of Saskatchewan, Saskatoon, Canada
168. D. J. Zaffarano, Physics Department, Iowa State University, Ames, Iowa
169. H. E. Johns, University of Saskatchewan, Saskatoon, Canada
170. J. Kastner, Argonne National Laboratory, 9700 South Cass Avenue, Argonne, Illinois

171. J. Arol Simpson, National Bureau of Standards, Washington, D.C.
172. L. M. Langer, Physics Department, University of Indiana, Bloomington, Indiana
173. C. S. Wu, Physics Department, Columbia University, New York, New York
174. C. E. Klots, Florida State University, Tallahassee, Florida
175. V. B. Bhanot, Physics Department, Panjab University, Chandigarh-3, India
176. Jacobo Rapaport, University of Chile, Box 2777, Institute of Science, Santiago, Chile
177. Research and Development Division, AEC, ORO
178-815. Given distribution as shown in TID-4500 (29th ed.) under Physics category (75 copies – OTS)